Supporting Information for

Stability of Metal–Metal Interactions in Transmetallation Intermediates Based on Electronics of Bridging Arene Ligands Determined Through Pyridine Titrations

Rana Marghalani, Eric S. Cueny*

Department of Chemistry, Boston University, 590 Commonwealth Ave., Boston, Massachusetts 02215, United States

Corresponding Author

*ecueny@bu.edu

Contents

General Experimental Considerations

The solvents and reagents were used as received unless otherwise noted. The compounds **1**,[1] **1-F**,[1] and **2**[2] were synthesized according to literature procedures. All NMR spectroscopic data were collected using a Bruker Avance Neo 600 MHz NMR spectrometer equipped with a BBFO SmartProbe. All NMR spectra are recorded in ppm and referenced to residual proteo solvent resonances. High resolution mass spectrometry data were collected on a Waters QTof Premier. CV data were collected using a Pine WaveDriver 200 and were referenced to the ferrocene/ferrocenium redox couple, which was added after scan rate dependent studies were performed.

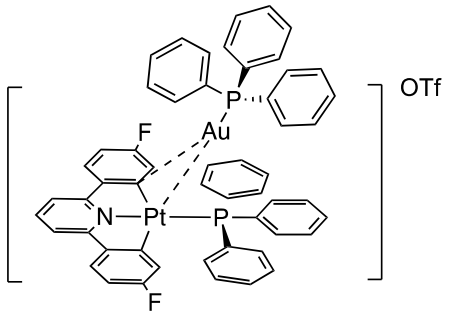

2-F

Synthesis of [(CNC^{F})(PPh_3)Pt–Au(PPh_3)][OTf] (2-F)

To a solution of Au(PPh_3)Cl (0.0205g, 0.0415 mmol) in THF (1 ml), AgOTf (0.0107 g, 0.0415 mmol) was added and the solution left to stir for 10 mins in the dark. The resulting solution was then filtered through Celite to remove AgCl salts. Compound **1-F** (0.0300 g, 0.0415 mmol) was added to the solution of [(PPh_3)Au][OTf] and stirred for 30 mins in the dark. THF solvent is then removed *in vacuo* to obtain a red-orange solid. The solid is then recrystallized by slow diffusion of pentane into a DCM solution of **2-F** (yield: 0.0331 g, 60 %). Bulk purity of this compound was established via a potency test using quantitative ^{1}H NMR spectroscopy (*vide infra*) to yield a potency of 95.2 %. ^{1}H NMR (600 MHz, CD_2Cl_2) δ 7.91 (t, *J* = 8.0 Hz, 1H), 7.79 – 7.46 (m, 8H), 7.61 – 7.46 (m, 8H), 7.34 (td, *J* = 7.8, 2.7 Hz, 6H), 7.23 (td, *J* = 7.8, 2.5 Hz, 6H), 7.09 (dd, *J* = 13.5, 7.7 Hz, 6H), 6.91 (td, *J* = 8.4, 4.9 Hz, 2H), 5.68 (d, *J* = 9.6 Hz, 2H). ^{31}P{^{1}H} NMR (243 MHz, CD_2Cl_2) δ 33.84 (s, $^{2}J_{P–Pt}$ = 267.2 Hz), 21.51 (s, $^{1}J_{P–Pt}$= 3568.25 Hz). ^{19}F{^{1}H} NMR (565 MHz, CD_2Cl_2) δ -78.90, -108.27. ^{13}C{^{1}H} NMR (151 MHz, CD_2Cl_2) δ 164.55, 164.15, 162.87, 150.12, 149.54, 143.20, 135.82 (d, *J* = 11.4 Hz), 133.95 (d, *J* = 13.8 Hz), 132.77 (d, *J* = 2.9 Hz), 132.48, 129.84 (d, *J* = 11.9 Hz), 129.27 (d, *J* = 11.3 Hz), 128.73, 128.33, 127.44, 121.47 (q, *J* = 324.3 Hz), 117.34, 116.50. HRMS (ESI): *m/z* calc for $C_{53}H_{39}AuF_2NP_2Pt$ (i.e. the cationic portion of **2-F**) 1181.1839; found, 1181.1891.

General procedure for pyridine and 2-fluoropyridine titration experiments

Complex **2-F** (0.0100g, 0.00751 mmol) was dissolved in CD_2Cl_2 and 2-fluoropyridine (0.2 μL, ~ 0.36 eq) was added to the NMR sample using a 5 μL Hamilton syringe. Then, ^{1}H, ^{19}F, and ^{31}P NMR spectra were collected. Next, an additional 0.2 μL of 2-fluoropyridine was added to the NMR sample followed by collection of ^{1}H, $^{19}F\{^{1}H\}$, and $^{31}P\{^{1}H\}$ NMR spectra. This process was repeated for a total of 10 additions of 2-fluoropyridine to the NMR solution of **2-F** (*vide infra*) Due to the small quantities of titrant (0.2 μL) added in these experiments, the actual ratio of 2-fluoropyridine to **2-F** was determined by integration of the ^{1}H NMR spectra.
A nearly identical procedure was carried out for pyridine titrations with **2-F,** 2-fluoropyridine titrations with **2**, and pyridine titrations with **2**.

General procedure for CV experiments

For CV experiments, a glassy carbon electrode was used as the working electrode, platinum wire was used as the counter electrode, and a silver wire reference electrode was used. The working electrode was polished prior to each CV experiment. A solution of electrolyte (100 mM tetrabutyl ammonium hexafluorophosphate in DCM) was prepared. Background scans were taken of the electrolyte solution prior to addition of the desired complexes. Then, complex **1** or **1-F** was added to the solution to yield a concentration of 0.28 mM. One scan each was taken at the following scan rates: 1000, 500, 250, 100, 50, 25, 10 mV/s. Following scan rate dependent studies, ferrocene was added to the solution and a final scan collected for reference.

Procedure for potency test of 2-F

Here, a potency test by ^{1}H NMR spectroscopy (using an internal standard) was used to determine purity of **2-F**.[3–7] An NMR sample of **2-F** (0.0080g, 0.00601 mmol) was prepared by dissolving in CD_2Cl_2. Then, 1 μL (0.00941 mmol) of toluene was added to the NMR tube to serve as the internal standard and a ^{1}H NMR spectrum was collected (D_1= 30s). Three peaks associated with complex **2-F** were integrated and the concentration determined relative to added internal standard using the toluene methyl peak. The potency based on three different peaks of **2-F** were calculated to be 99.4%, 92.4%, and 93.9%. The three potency values were averaged to give 95.2% potency of **2-F** in solution.

NMR spectra of 2-F

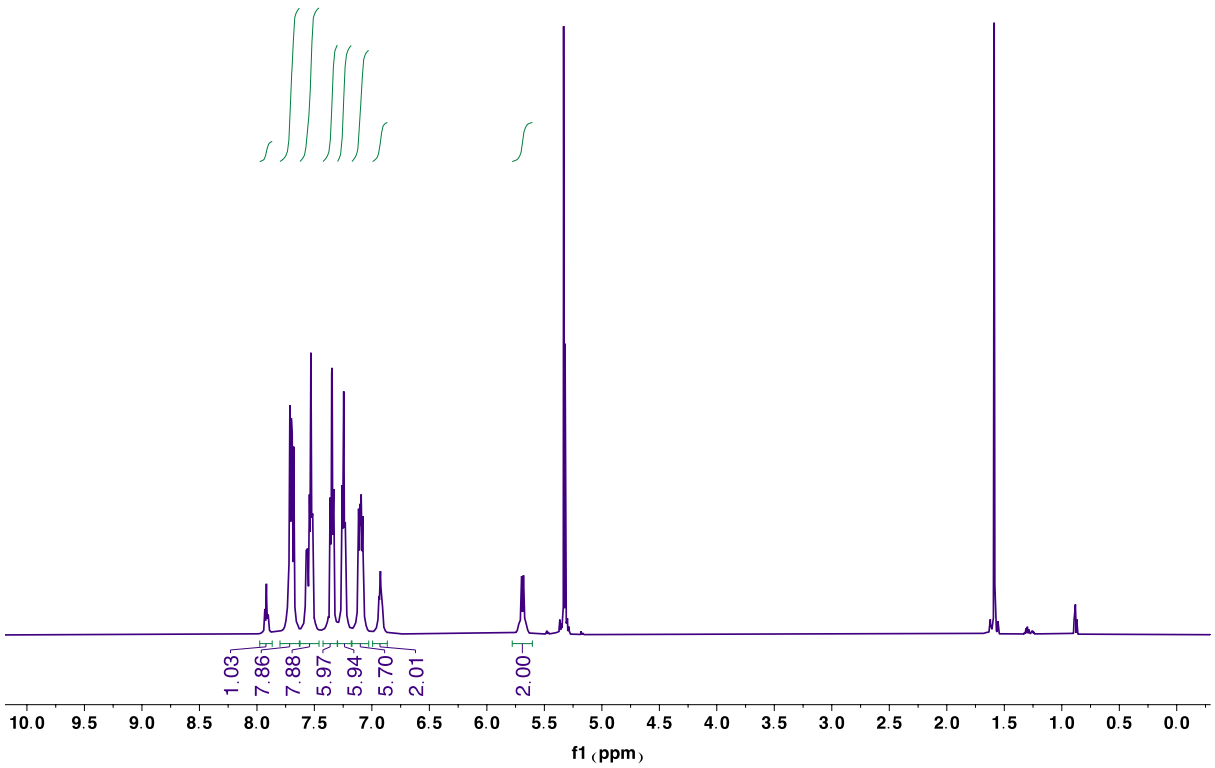

Figure S1. ^{1}H NMR spectrum of **2-F** in CD_2Cl_2.

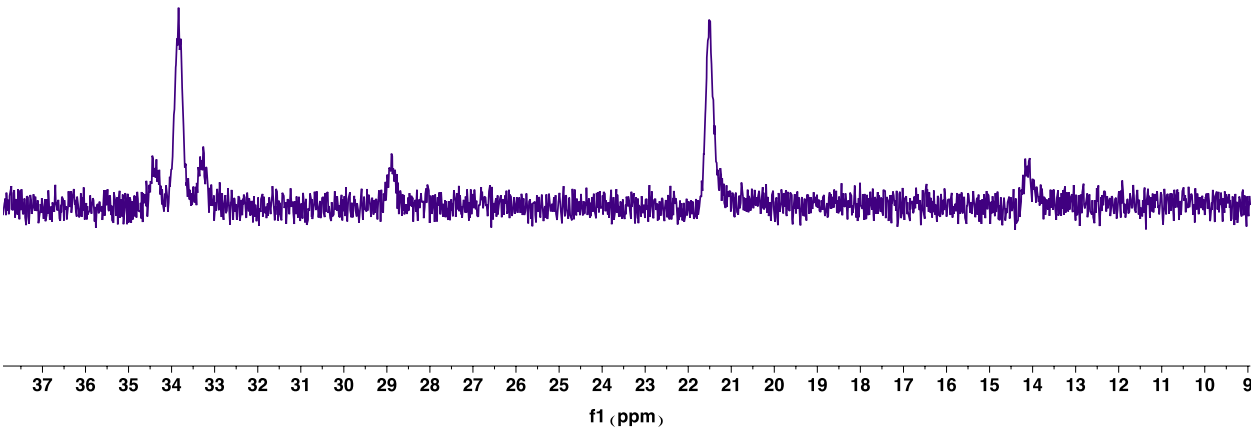

Figure S2. $^{31}P\{^{1}H\}$ NMR spectrum of **2-F** in CD_2Cl_2.

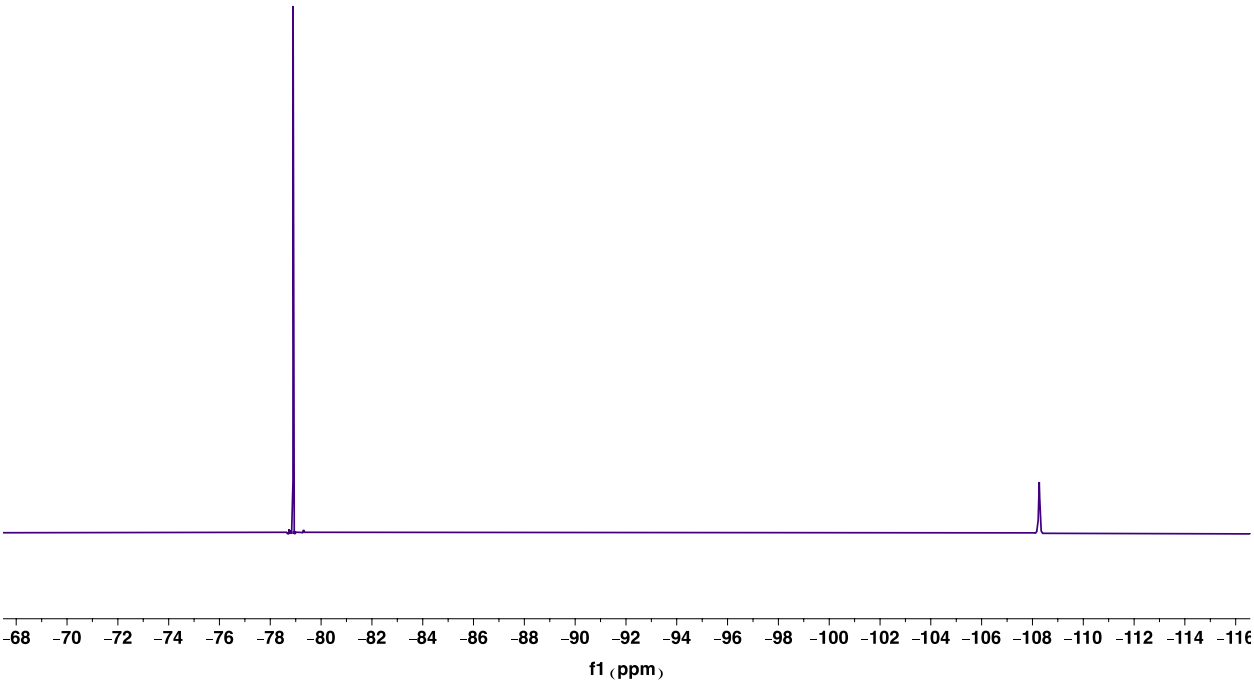

Figure S3. $^{19}F\{^{1}H\}$ NMR spectrum of **2-F** in CD_2Cl_2

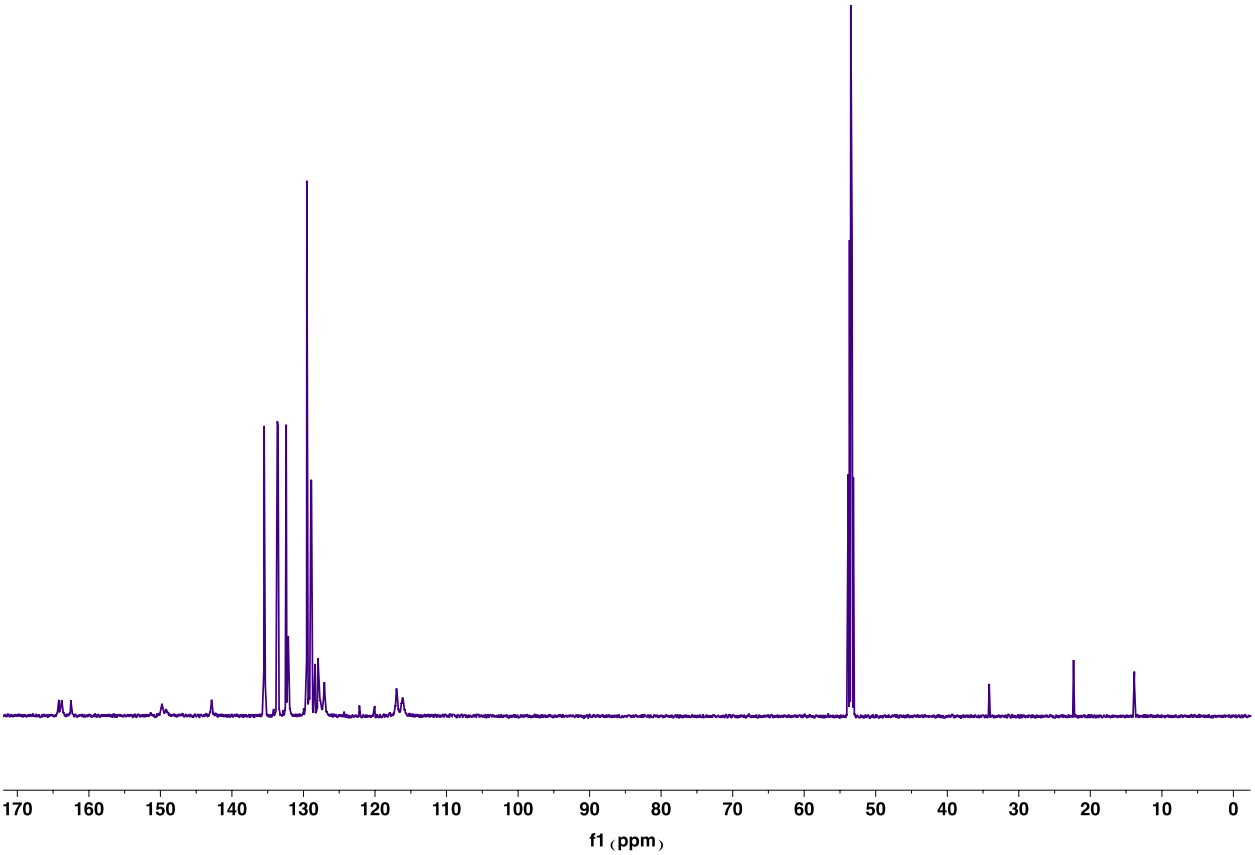

Figure S4. $^{13}C\{^{1}H\}$ NMR spectrum of **2-F** in CD_2Cl_2. Residual pentane (from recrystallization) observed in the spectrum.

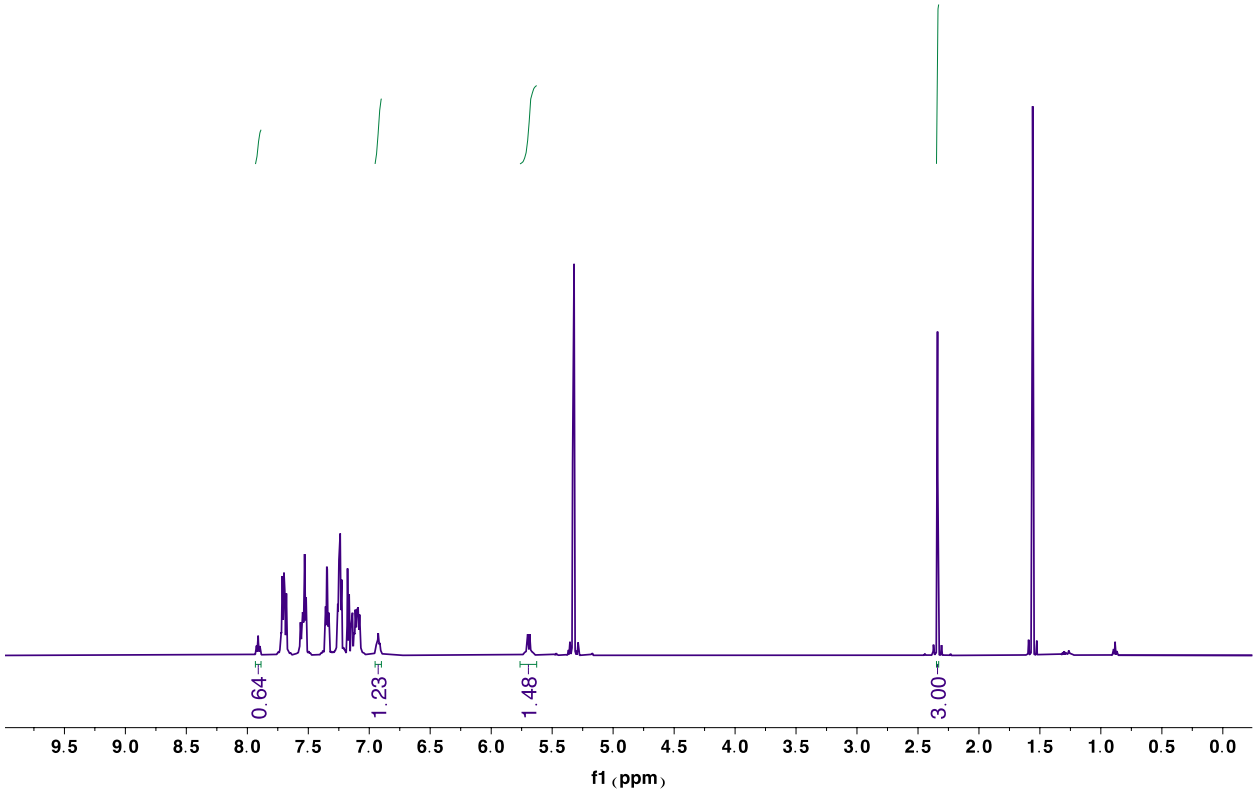

Figure S5. ^{1}H NMR spectrum of **2-F** used for the potency test (*vide infra*).

NMR spectra of 2-fluoropyridine titrations with 2-F

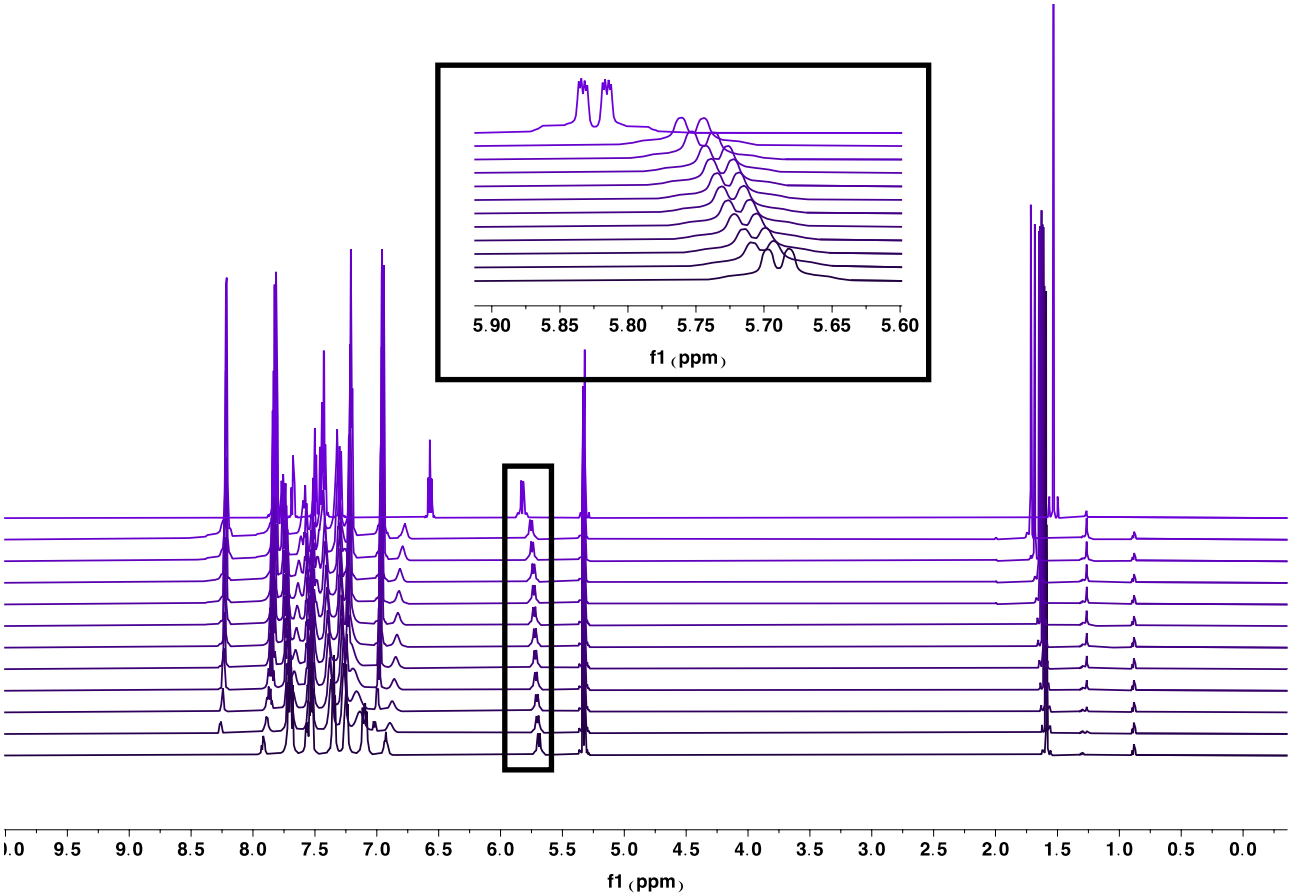

Figure S6. ^{1}H NMR spectra of titration experiments with 2-fluoropyridine and **2-F** (0.0100g, 0.00751 mmol) in CD_2Cl_2. Bottom ^{1}H NMR spectrum is **2-F** in the absence of 2-fluoropyridine. Top ^{1}H NMR spectrum is **1-F** in the absence of 2-fluoropyridine. The second spectrum up from the bottom to the second to last spectrum from the top in ascending order are the titrations of 2-fluoropyridine with 0.095 eq, 0.19 eq, 0.27 eq, 0.38 eq, 0.65 eq, 0.89 eq, 1.16 eq, 1.31 eq, 2.10 eq, 2.77 eq relative to **2-F**. The box highlights peaks associated with the proton alpha to Pt in complex **2-F**.

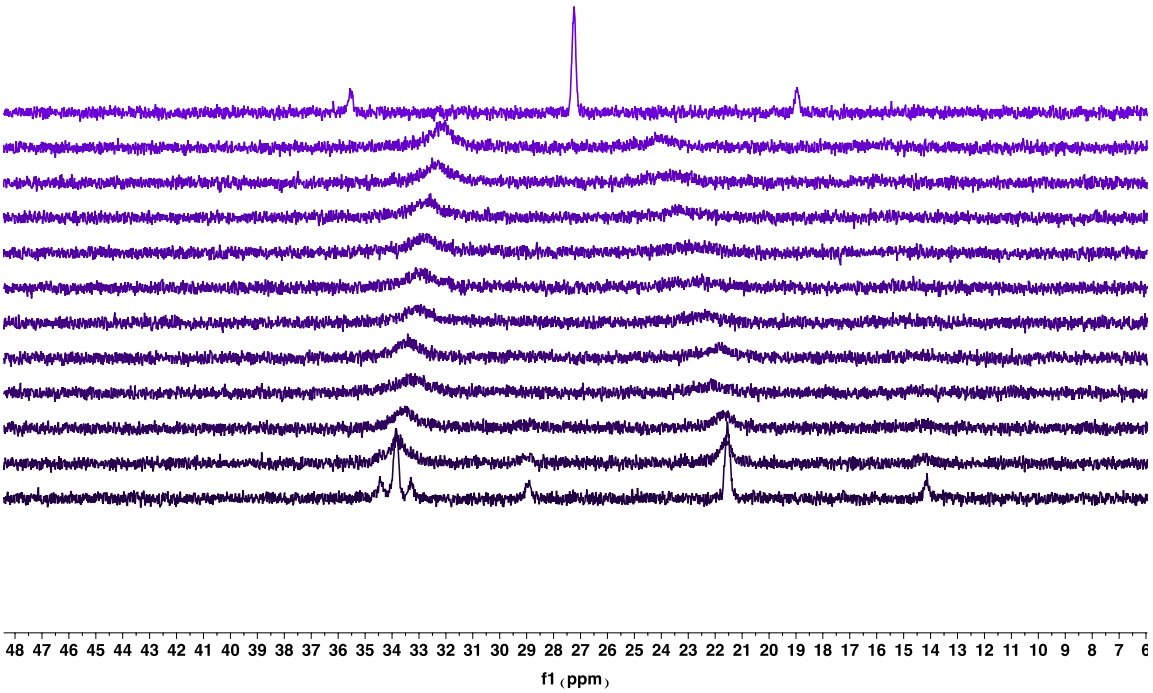

Figure S7. $^{31}P\{^{1}H\}$ NMR spectra of titration experiments with 2-fluoropyridine and **2-F** in CD_2Cl_2. Bottom $^{31}P\{^{1}H\}$ NMR spectrum is **2-F** in the absence of 2-fluoropyridine. Top $^{31}P\{^{1}H\}$ NMR spectrum is **1-F** in the absence of 2-fluoropyridine. From the second spectrum up from the bottom to the second to last spectrum from the top in ascending order are the titrations of 2-fluoropyridine in with 0.095 eq, 0.19 eq, 0.27 eq, 0.38 eq, 0.65 eq, 0.89 eq, 1.16 eq, 1.31 eq, 2.10 eq, 2.77 eq relative to **2-F**.

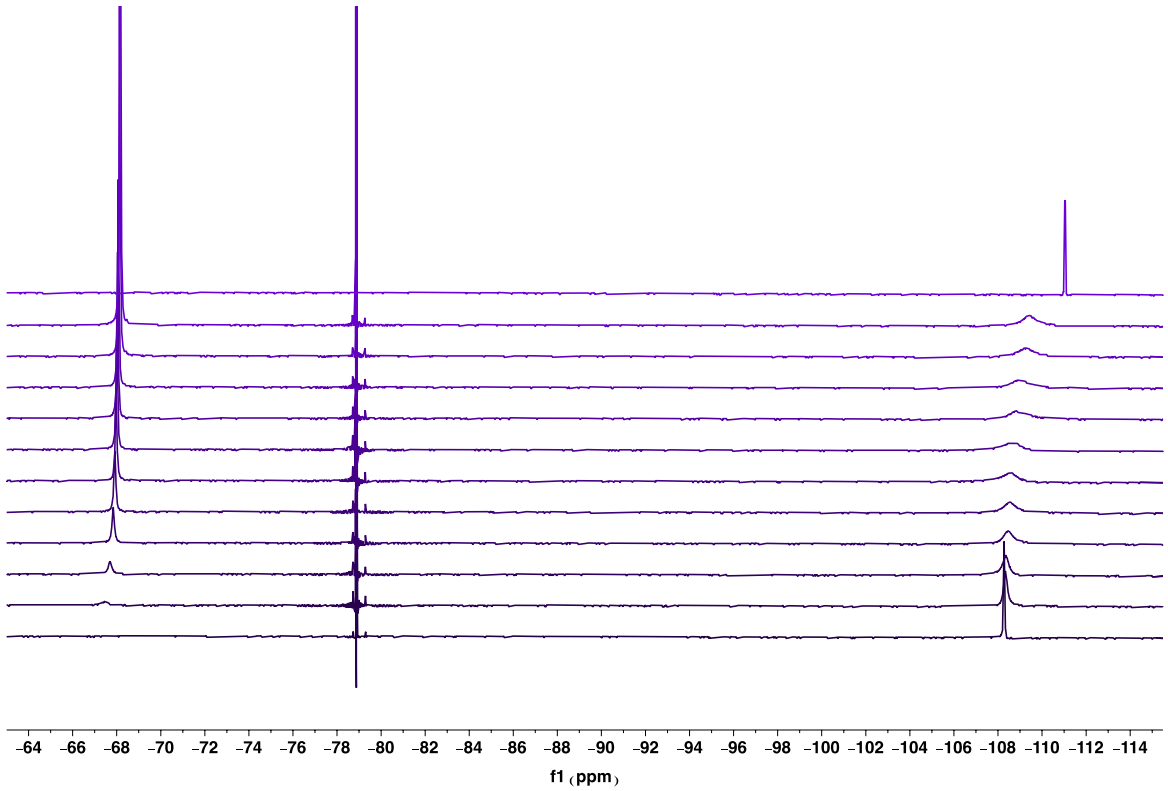

Figure S8. $^{19}F\{^{1}H\}$ NMR spectra of titration experiment with 2-fluoropyridine and **2-F** in CD_2Cl_2. Bottom $^{19}F\{^{1}H\}$ NMR spectrum is **2-F** in the absence of 2-fluoropyridine. Top $^{19}F\{^{1}H\}$ NMR spectrum is **1-F** in the absence of 2-fluoropyridine. From the second spectrum up from the bottom to the second to last spectrum from the top in ascending order are the titrations of 2-fluoropyridine in with 0.095 eq, 0.19 eq, 0.27 eq, 0.38 eq, 0.65 eq, 0.89 eq, 1.16 eq, 1.31 eq, 2.10 eq, 2.77 eq relative to **2-F**.

NMR spectra of pyridine titrations with 2-F

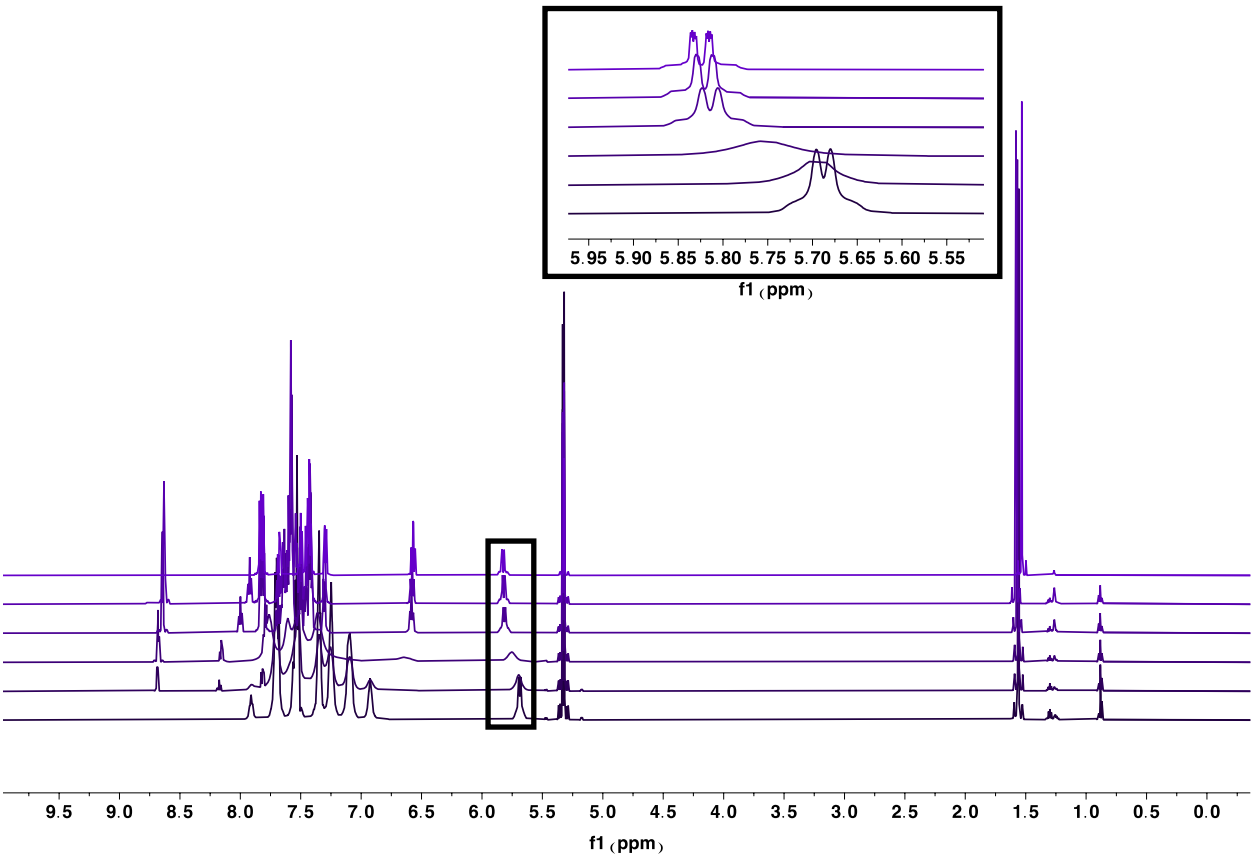

Figure S9. ^{1}H NMR spectra of titration experiments with pyridine and **2-F** (0.0100g, 0.00751 mmol) in CD_2Cl_2. Bottom ^{1}H NMR spectrum is **2-F** in the absence of pyridine. Top ^{1}H NMR spectrum is **1-F** in the absence of pyridine. From the second spectrum up from the bottom to the second to last spectrum from the top in ascending order are the titrations of pyridine with 0.57 eq, 0.95 eq, 1.14 eq, 1.33 eq relative to **2-F**. The box highlights peaks associated with the proton alpha to Pt in complex **2-F**.

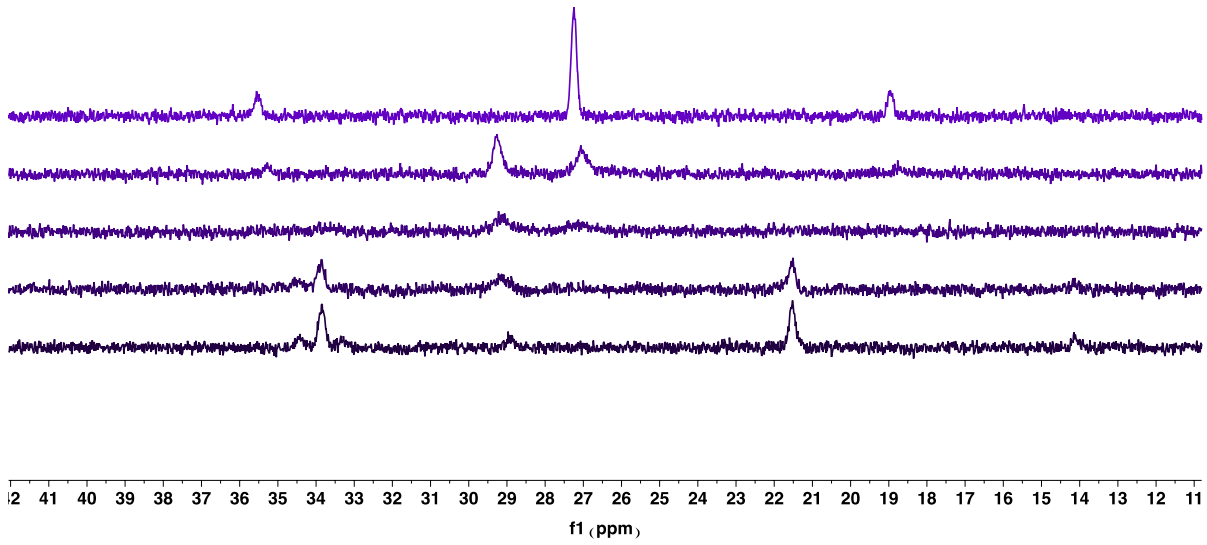

Figure S10. $^{31}P\{^{1}H\}$ NMR spectra of titration experiments with pyridine and **2-F** in CD_2Cl_2. Bottom $^{31}P\{^{1}H\}$ NMR spectrum is **2-F** in the absence of pyridine. Top $^{31}P\{^{1}H\}$ NMR spectrum is **1-F** in the absence of pyridine. From the second spectrum up from the bottom to the second to last spectrum from the top in ascending order are the titrations of pyridine with 0.57 eq, 0.95 eq, 1.14 eq, 1.33 eq relative to **2-F**.

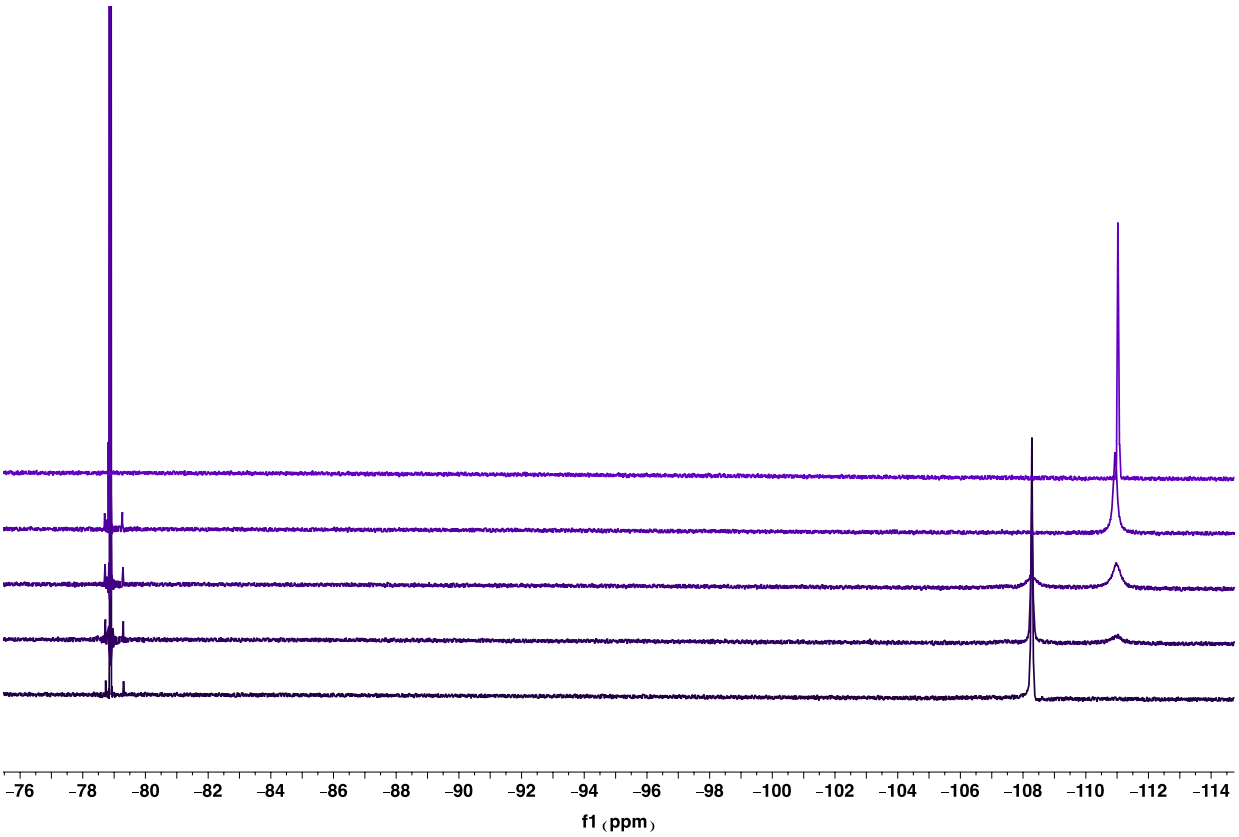

Figure S11. $^{19}F\{^{1}H\}$ NMR spectra of titration experiments with pyridine and **2-F** in CD_2Cl_2. Bottom $^{19}F\{^{1}H\}$ NMR spectrum is **2-F** in the absence of pyridine. Top $^{19}F\{^{1}H\}$ NMR spectrum is **1-F** in the absence of pyridine. From the second spectrum up from the bottom to the second to last spectrum from the top in ascending order are the titrations of pyridine in with 0.57 eq, 0.95 eq, 1.14 eq, 1.33 eq relative to **2-F**.

NMR spectra of 2-fluoropyridine titrations with 2

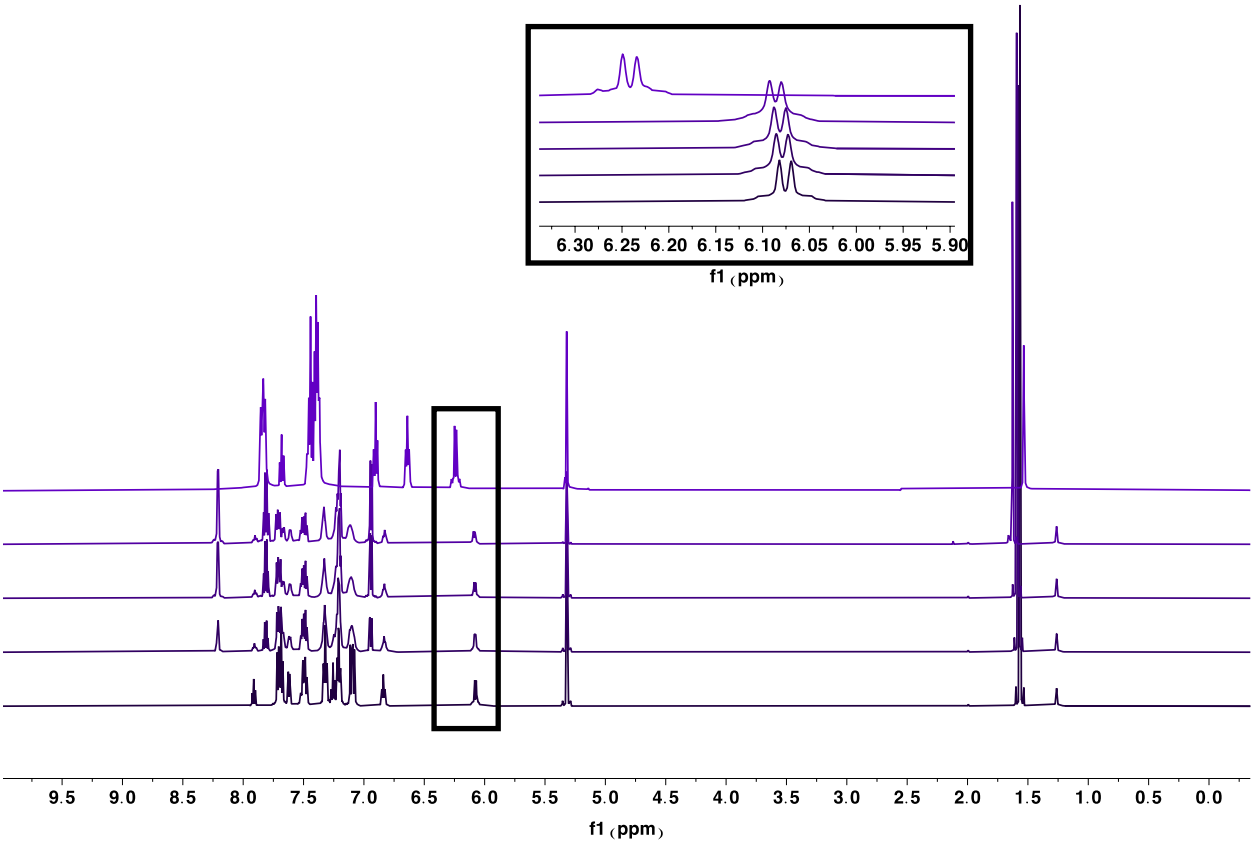

Figure S12. ^{1}H NMR spectra of titration experiments with 2-fluoropyridine and **2** (0.0053 g, 0.00409 mmol) in CD_2Cl_2. Bottom ^{1}H NMR spectrum is **2** in the absence of 2-fluoropyridine. Top ^{1}H NMR spectrum is **1** in the absence of 2-fluoropyridine. From the second spectrum up from the bottom to the second to last spectrum from the top in ascending order are the titrations of pyridine with 0.61 eq, 1.25 eq, 2.01 eq relative to **2**. The box highlights peaks associated with the proton alpha to Pt in complex **2**.

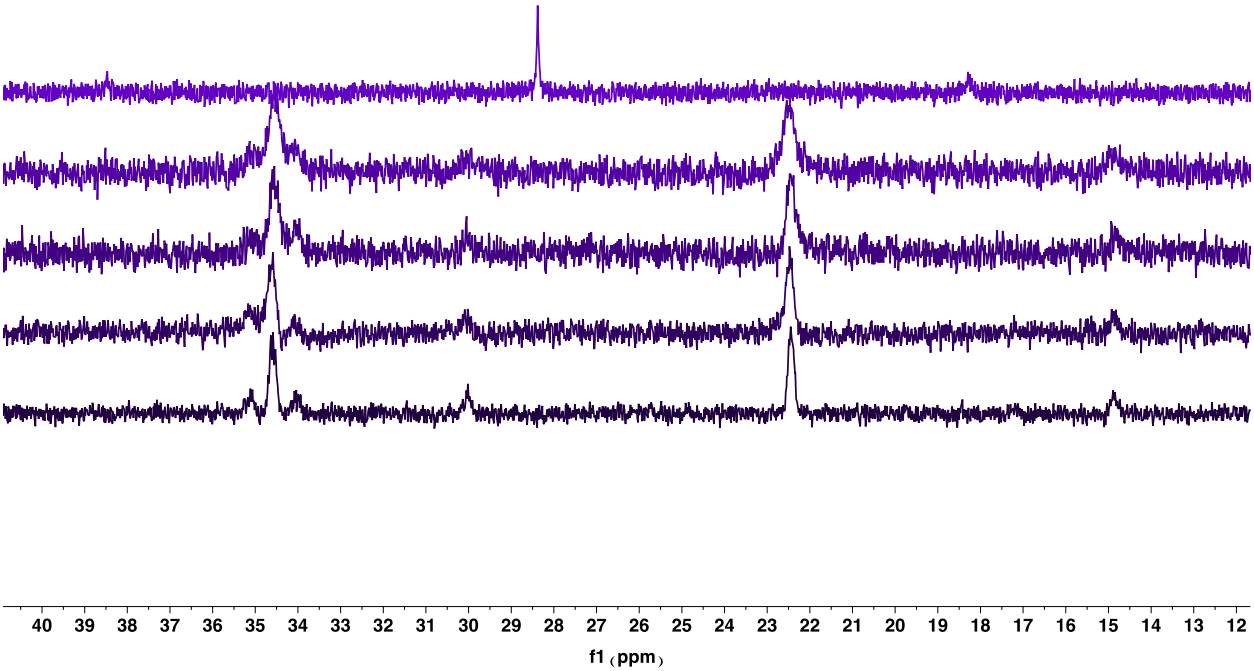

Figure S13. $^{31}P\{^{1}H\}$ NMR spectra of titration experiments with 2-fluoropyridine and **2** in CD_2Cl_2. Bottom $^{31}P\{^{1}H\}$ NMR spectrum is **2** in the absence of 2-fluoropyridine. Top $^{31}P\{^{1}H\}$ NMR spectrum is **1** in the absence of 2-fluoropyridine. From the second spectrum up from the bottom to the second to last spectrum from the top in ascending order are the titrations of pyridine in with 0.61 eq, 1.25 eq, 2.01 eq relative to **2**.

NMR spectra of pyridine titrations with 2

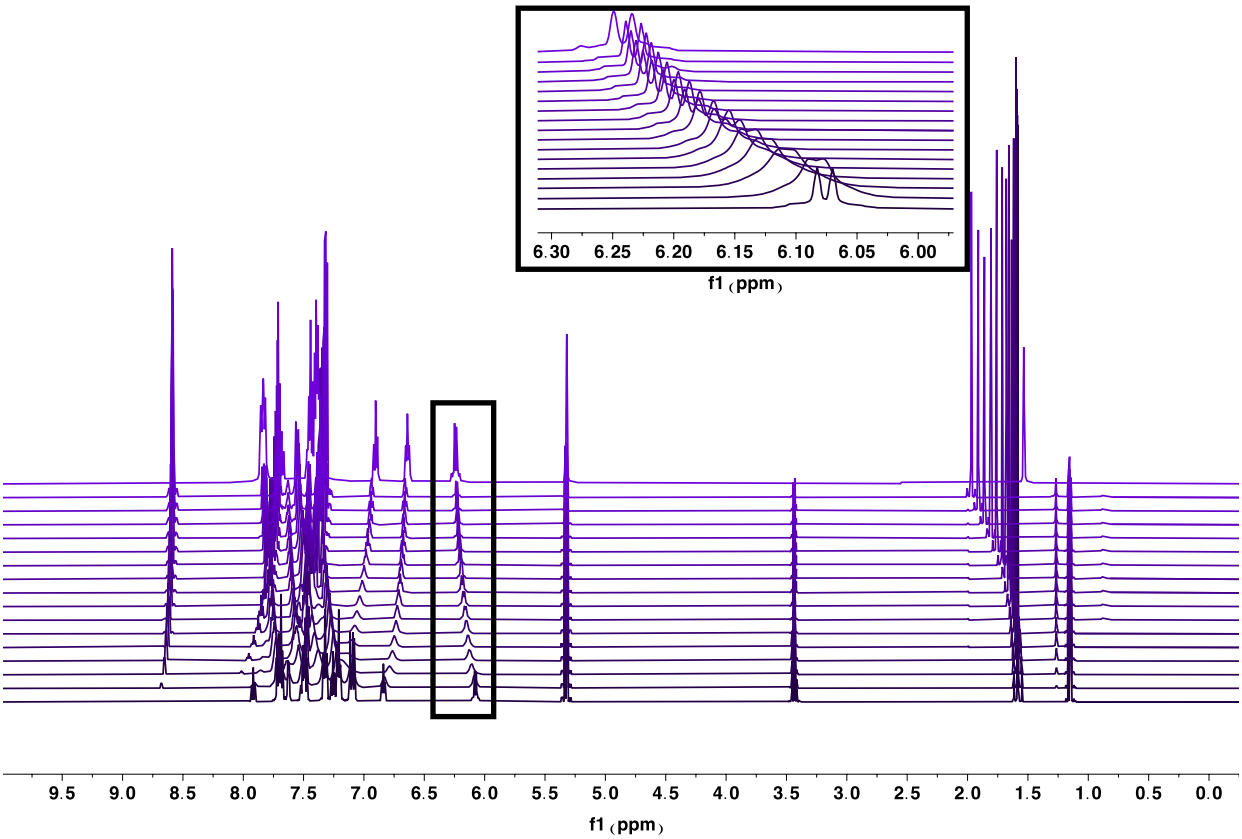

Figure S14. ^{1}H NMR spectra of titration experiments with pyridine and **2** (0.0086g, 0.00664 mmol) in CD_2Cl_2. Bottom ^{1}H NMR spectrum is **2** in the absence of pyridine. Top ^{1}H NMR spectrum is **1** in the absence of 2-fluoropyridine. From the second spectrum up from the bottom to the second to last spectrum from the top in ascending order are the titrations of pyridine with 0.10 eq, 0.35 eq, 0.60 eq, 0.83 eq, 1.13 eq, 1.40 eq, 1.91 eq, 2.47 eq, 3.05 eq, 3.96 eq, 5.21 eq, 6.51 eq, 8.29 eq, 9.64 eq, 11.54 eq relative to **2**. The box highlights peaks associated with the proton alpha to Pt in complex **2**.

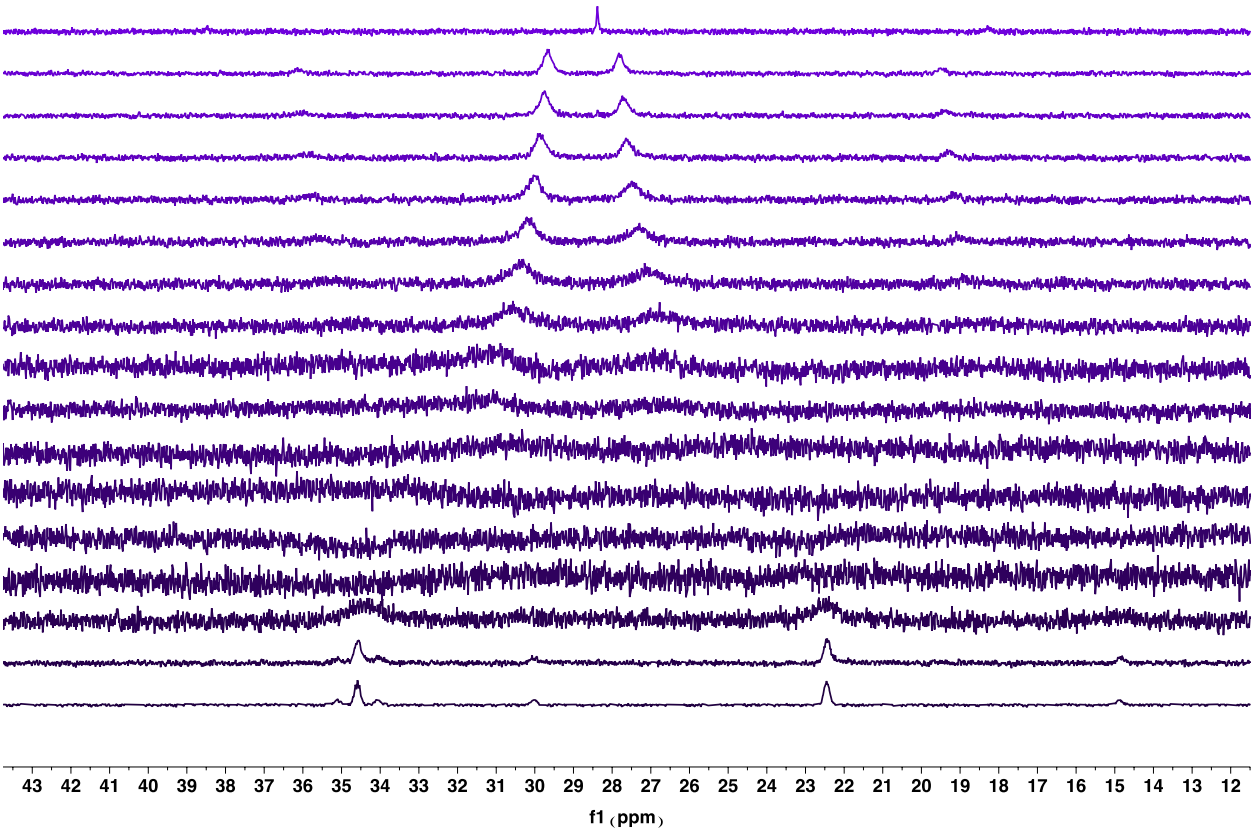

Figure S15. $^{31}P\{^{1}H\}$ NMR spectra of titration experiments with pyridine and complex **2** in CD_2Cl_2. Bottom $^{31}P\{^{1}H\}$ NMR spectrum is **2** in the absence of pyridine. Top $^{31}P\{^{1}H\}$ NMR spectrum is **1** in the absence of 2-fluoropyridine. From the second spectrum up from the bottom to the second to last spectrum from the top in ascending order are the titrations of pyridine with 0.10 eq, 0.35 eq, 0.60 eq, 0.83 eq, 1.13 eq, 1.40 eq, 1.91 eq, 2.47 eq, 3.05 eq, 3.96 eq, 5.21 eq, 6.51 eq, 8.29 eq, 9.64 eq, 11.54 eq relative to **2**.

NMR spectra of 2-fluoropyridine addition to 1-F

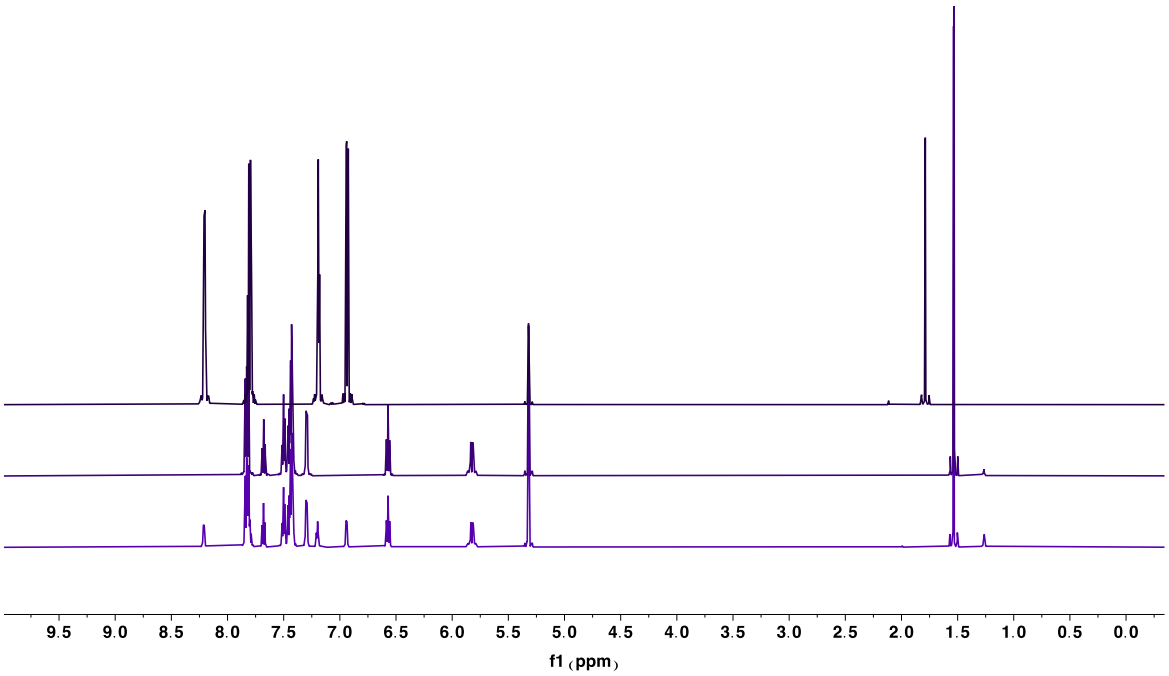

Figure S16. ^{1}H NMR spectra of the following in CD_2Cl_2: Bottom spectrum is **1-F** (0.0051 g, 0.00682 mmol) with 1 eq of 2-fluoropyridine. Middle spectrum is complex **1-F** in the absence of 2-fluoropyridine. Top spectrum is 2-fluoropyridine.

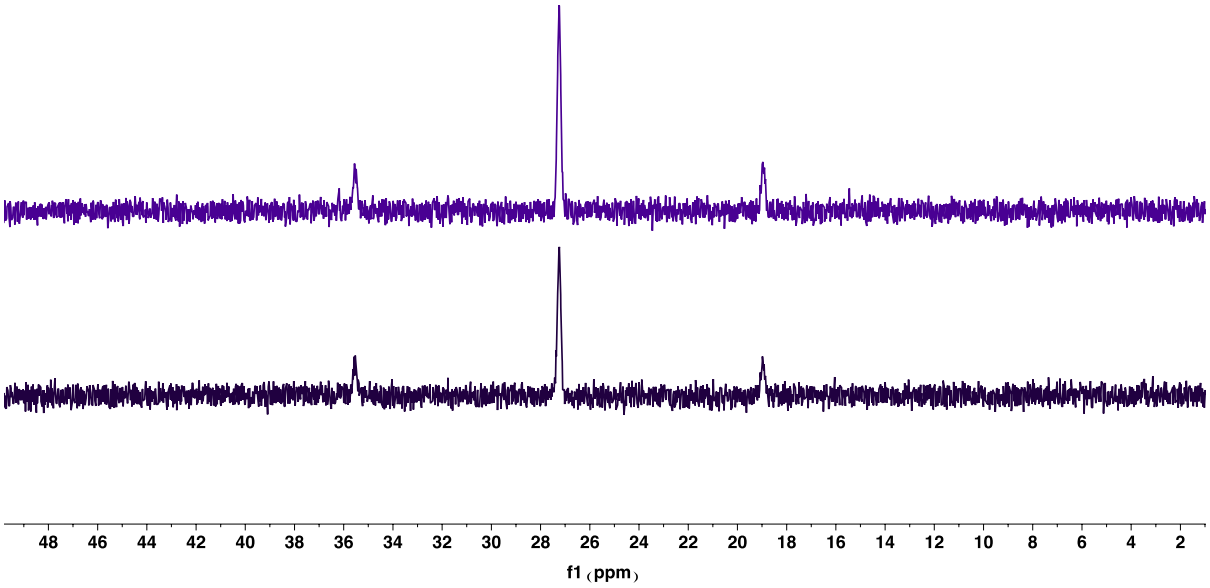

Figure S17. $^{31}P\{^{1}H\}$ NMR spectra of the following in CD_2Cl_2: Bottom spectrum is **1-F** with 1eq of 2-fluoropyridine. Top spectrum is complex **1-F** in the absence of 2-fluoropyridine.

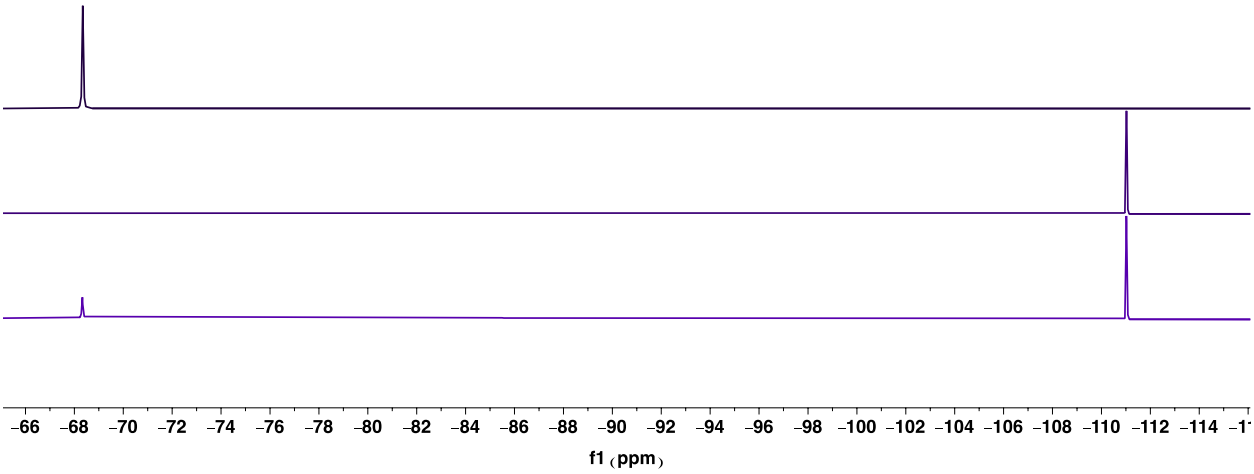

Figure S18. $^{19}F\{^{1}H\}$ NMR spectra of the following in CD_2Cl_2: Bottom spectrum is **1-F** with 1eq of 2-fluoropyridine. Middle spectrum is complex **1-F** in the absence of 2-fluoropyridine. Top spectrum is 2-fluoropyridine.

NMR spectra of pyridine addition to 1-F

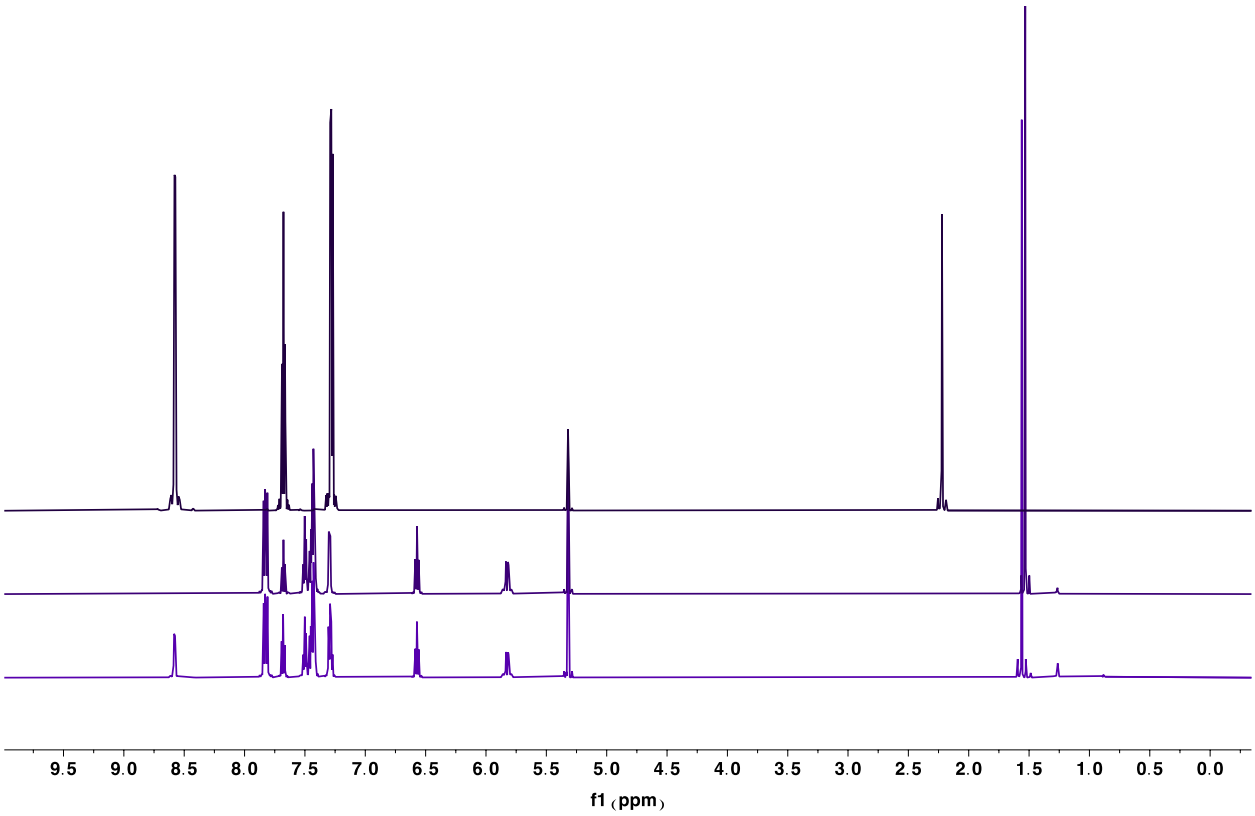

Figure S19. ^{1}H NMR spectra of the following in CD_2Cl_2: Bottom spectrum is **1-F** (0.0050 g, 0.00692 mmol) with 1eq of pyridine. Middle spectrum is **1-F** is the absence of pyridine. Top spectrum is pyridine**.**

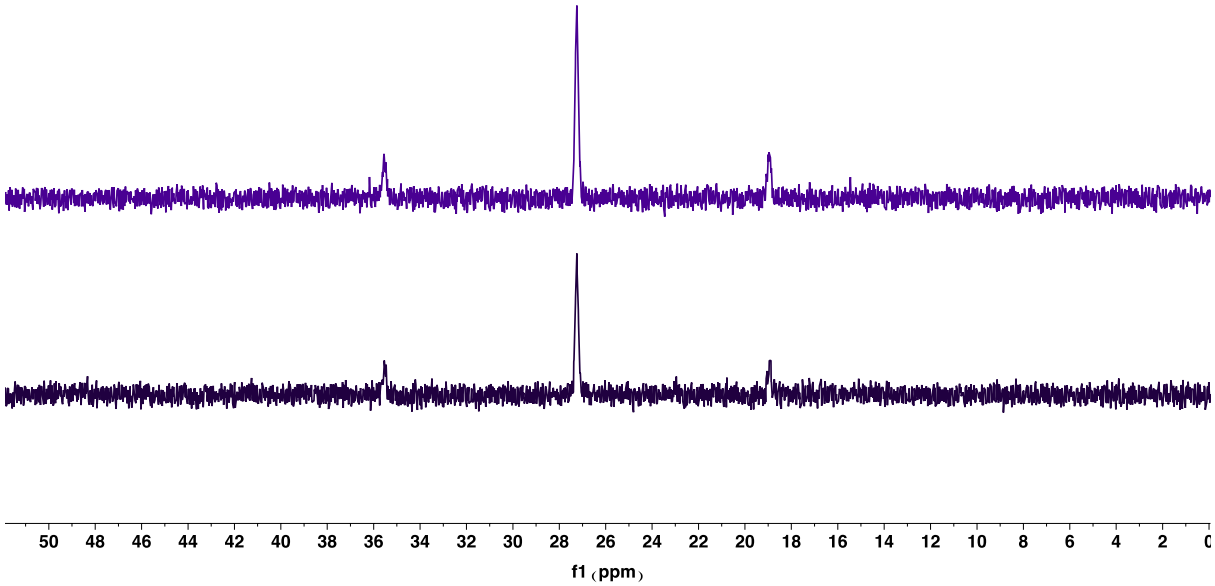

Figure S20. $^{31}P\{^{1}H\}$ NMR spectra of the following in CD_2Cl_2: Bottom spectrum is **1-F** with 1eq of pyridine. Top spectrum is of **1-F** is the absence of pyridine.

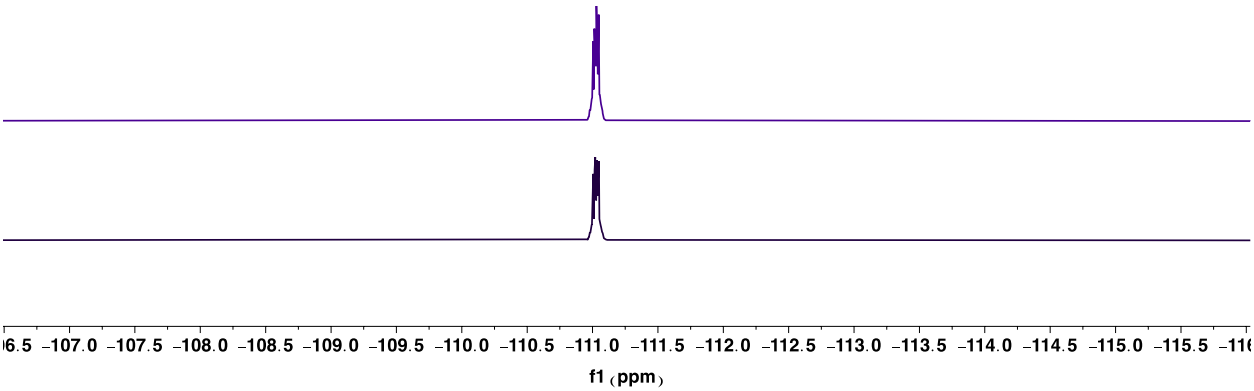

Figure S21. ^{19}F NMR spectra of the following in CD_2Cl_2: Bottom spectrum is **1-F** with 1eq of pyridine. Top spectrum is **1-F** is the absence of pyridine.

NMR spectra of 2-fluoropyridine addition to 1

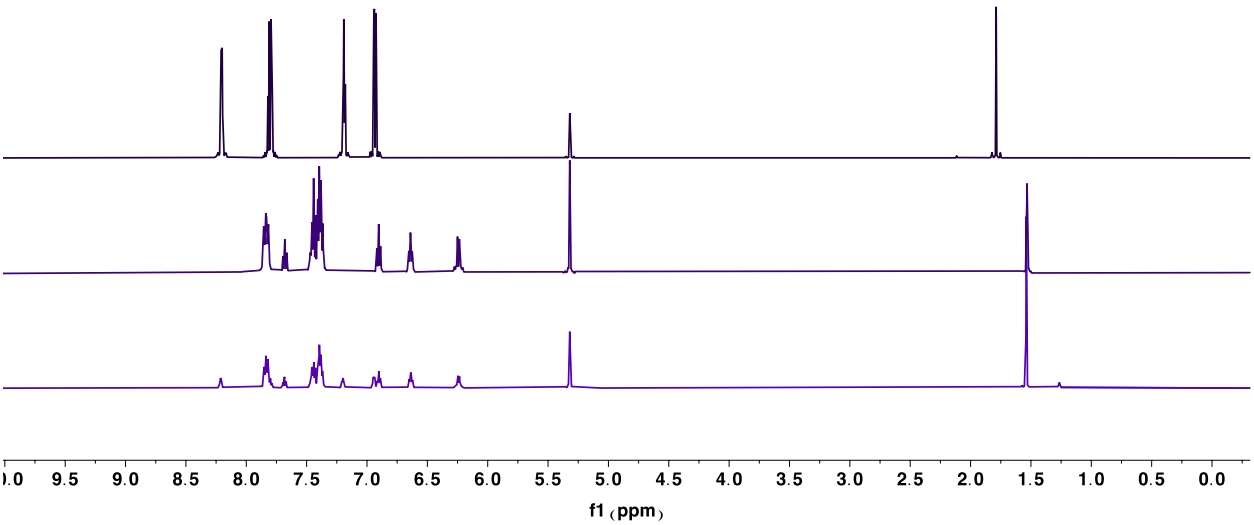

Figure S22. ^{1}H NMR spectra of the following in CD_2Cl_2: Bottom spectrum is **1** (0.0053 g, 0.00772 mmol) with 1eq of 2-fluoropyridine. Middle spectrum is **1** in the absence of 2-fluoropyridine. Top spectrum is 2-fluoropyridine.

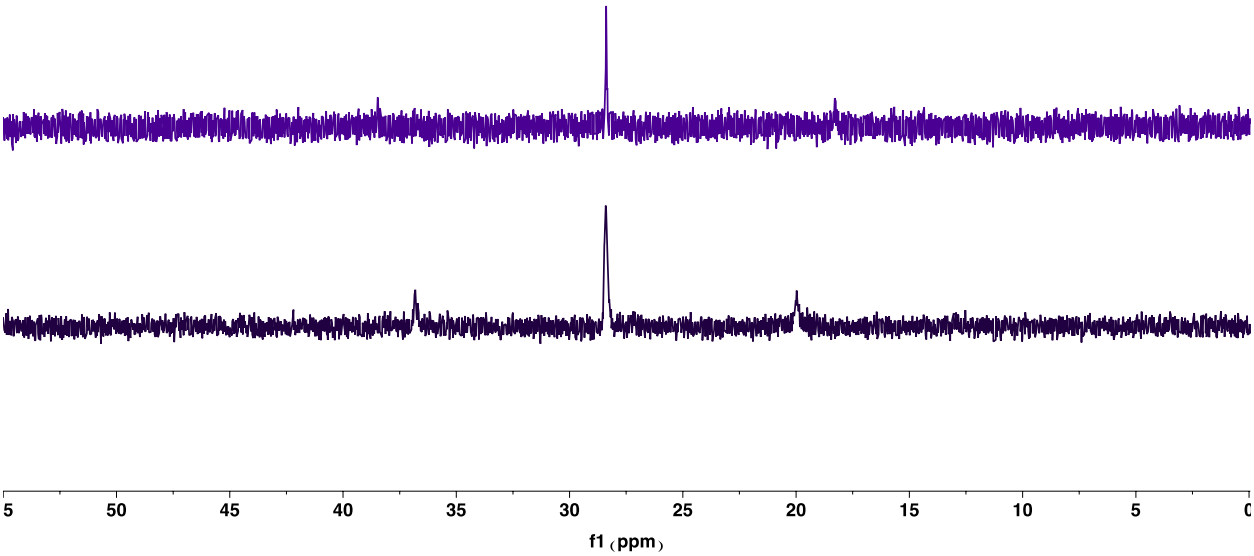

Figure S23. $^{31}P\{^{1}H\}$ NMR spectra of the following in CD_2Cl_2: Bottom spectrum is **1** with 1 eq of 2-fluoropyridine. Top spectrum is **1** in the absence of 2-fluoropyridine.

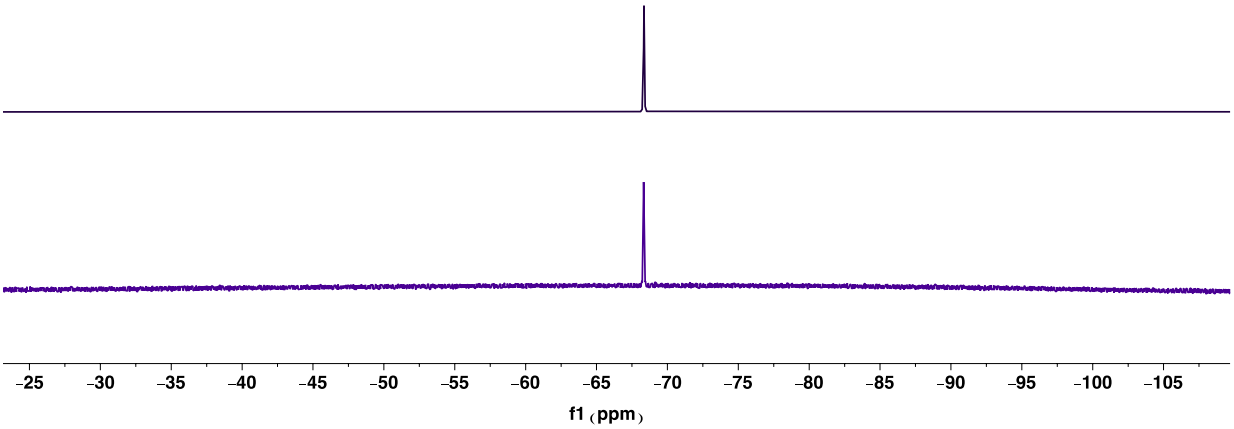

Figure S24. $^{19}F\{^{1}H\}$ NMR spectra of the following in CD_2Cl_2: Bottom spectrum is **1** with 1 eq of 2-fluoropyridine. Top spectrum is 2-fluoropyridine.

NMR spectra of pyridine addition to 1

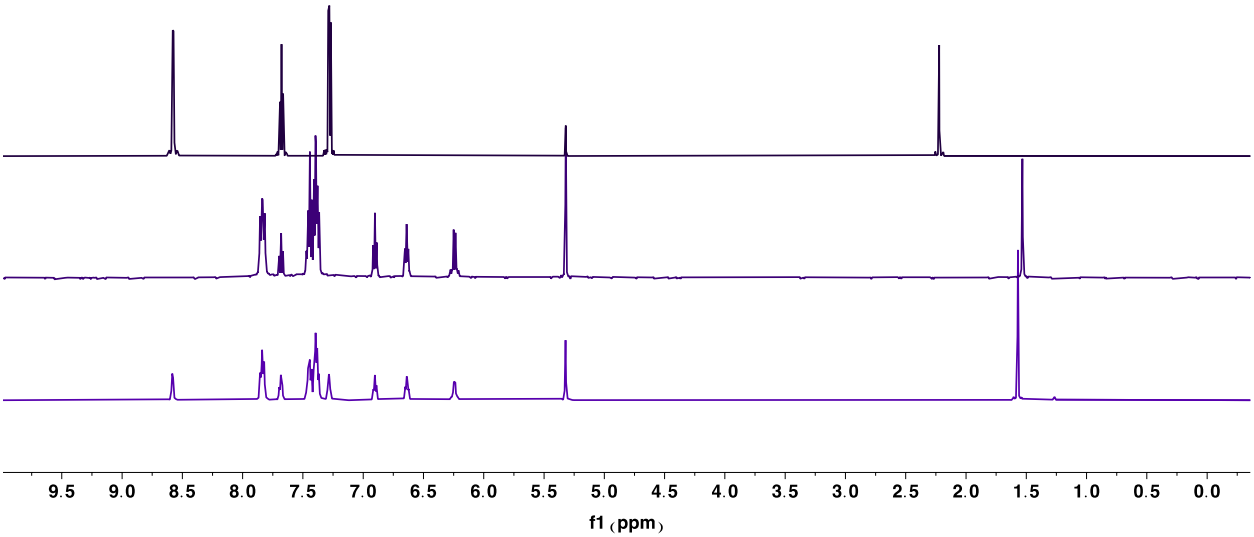

Figure S25. ^{1}H NMR spectra of the following in CD_2Cl_2: Bottom spectrum is **1** (0.0052 g, 0.00757 mmol) with 1 eq of pyridine. Middle spectrum is **1** is the absence of pyridine. Top spectrum is pyridine

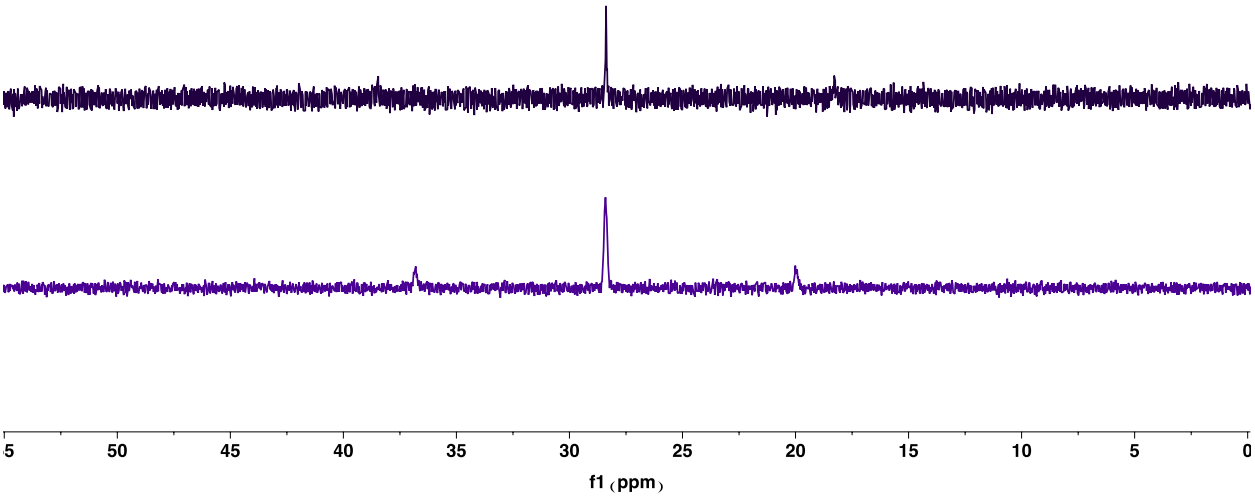

Figure S26. $^{31}P\{^{1}H\}$ NMR spectra of the following in CD_2Cl_2: Bottom spectrum is **1** with 1 eq of pyridine. Top spectrum is **1** in the absence of pyridine**.**

NMR spectra of 2-fluoropyridine addition to [(PPh_3)Au][OTf]

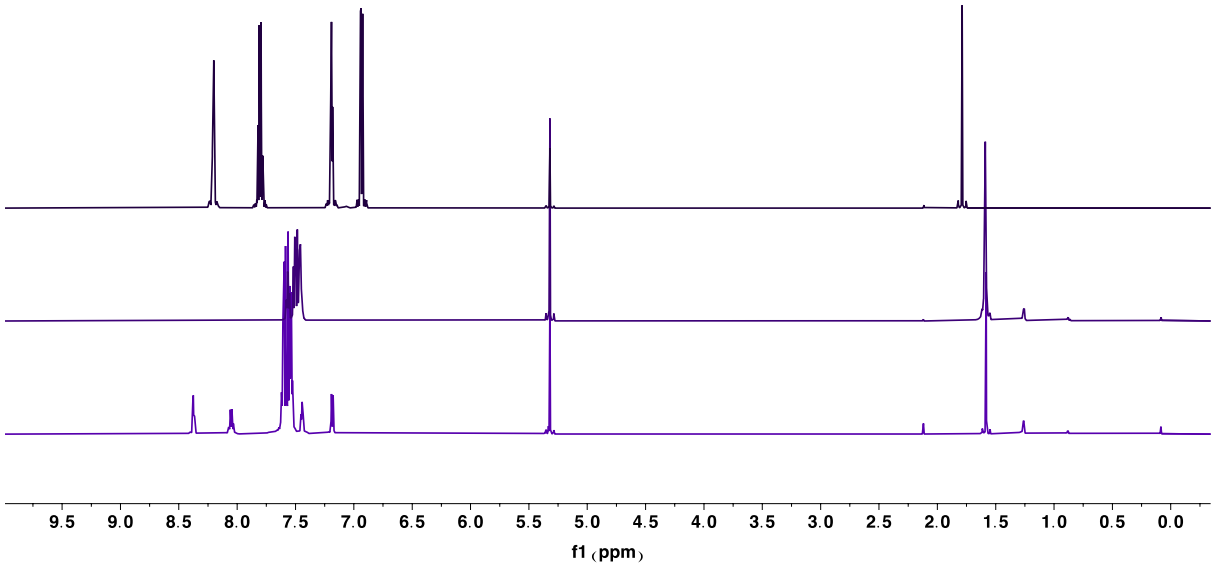

Figure S27. ^1H NMR spectra of the following in CD_2Cl_2: Bottom spectrum is [(PPh_3)Au][OTf] with 1 eq of 2-fluoropyridine. Middle spectrum is [(PPh_3)Au][OTf] in the absence of 2-fluoropyridine. Top spectrum is 2-fluoropyridine.

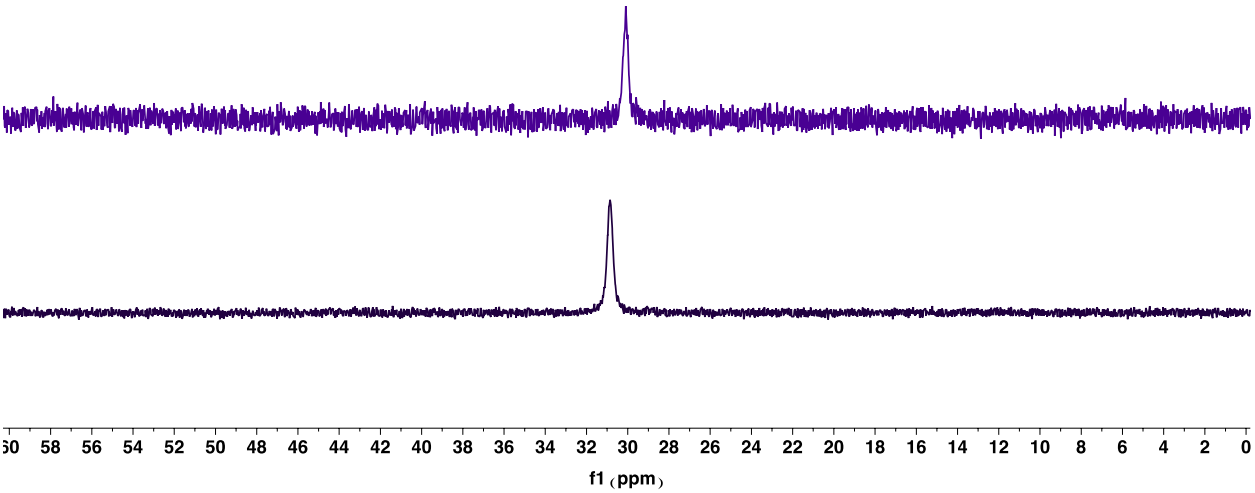

Figure S28. $^{31}P\{^{1}H\}$ NMR spectra of the following in CD_2Cl_2: Bottom spectrum is $[(PPh_3)Au][OTf]$ with 1 eq of 2-fluoropyridine. Top spectrum is $[Au(PPh_3)][OTf]$ in the absence of 2-fluoropyridine.

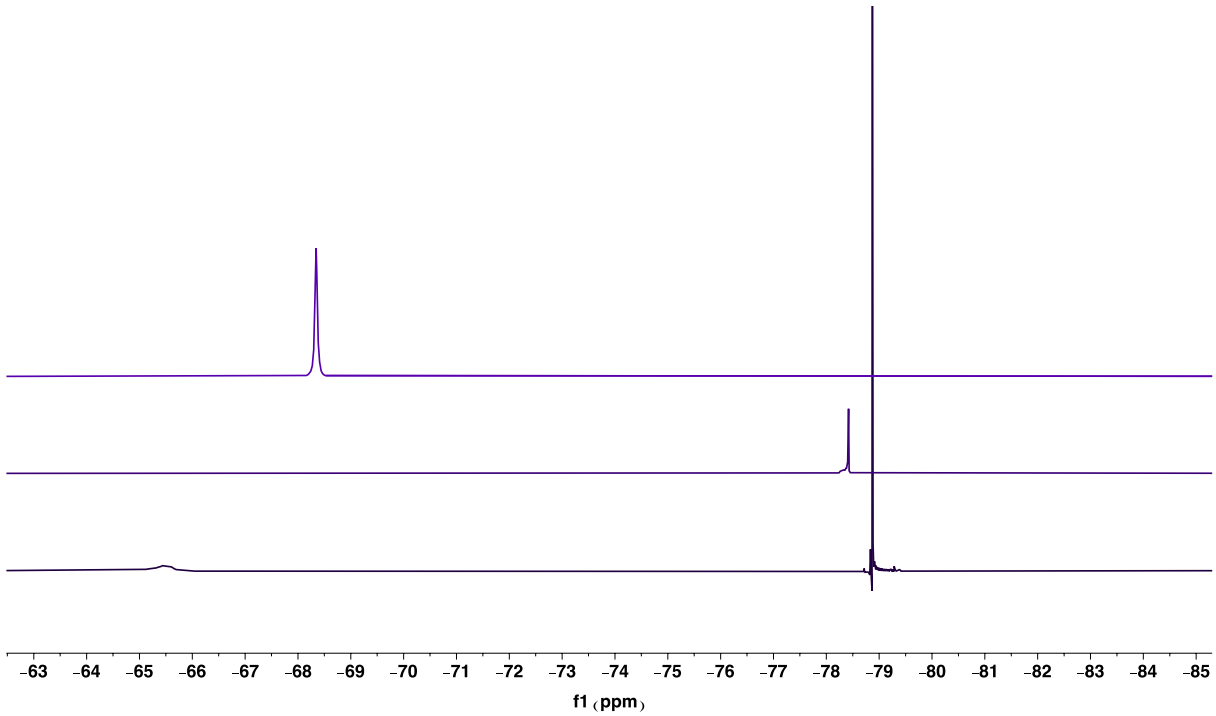

Figure S29. $^{19}F\{^{1}H\}$ NMR spectra of the following in CD_2Cl_2: Bottom spectrum is $[Au(PPh_3)][OTf]$ with 1 eq of 2-fluoropyridine. Middle spectrum is $[Au(PPh_3)][OTf]$ in the absence of 2-fluoropyridine. Top spectrum is 2-fluoropyridine.

NMR spectra of pyridine addition to [(PPh_3)Au][OTf]

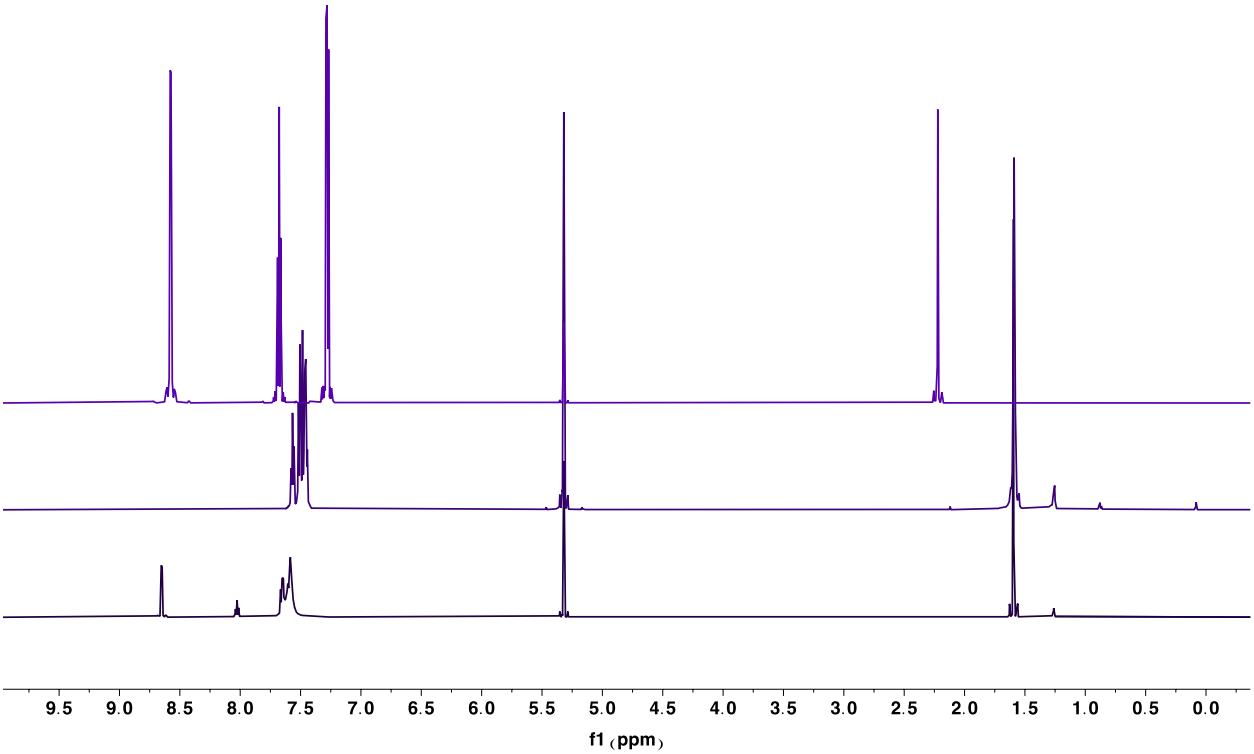

Figure S30. ^1H NMR spectra of the following in CD_2Cl_2: Bottom spectrum is [(PPh_3)Au][OTf] with 1 eq of pyridine. Middle spectrum is [(PPh_3)Au][OTf] in the absence of pyridine. Top spectrum is pyridine.

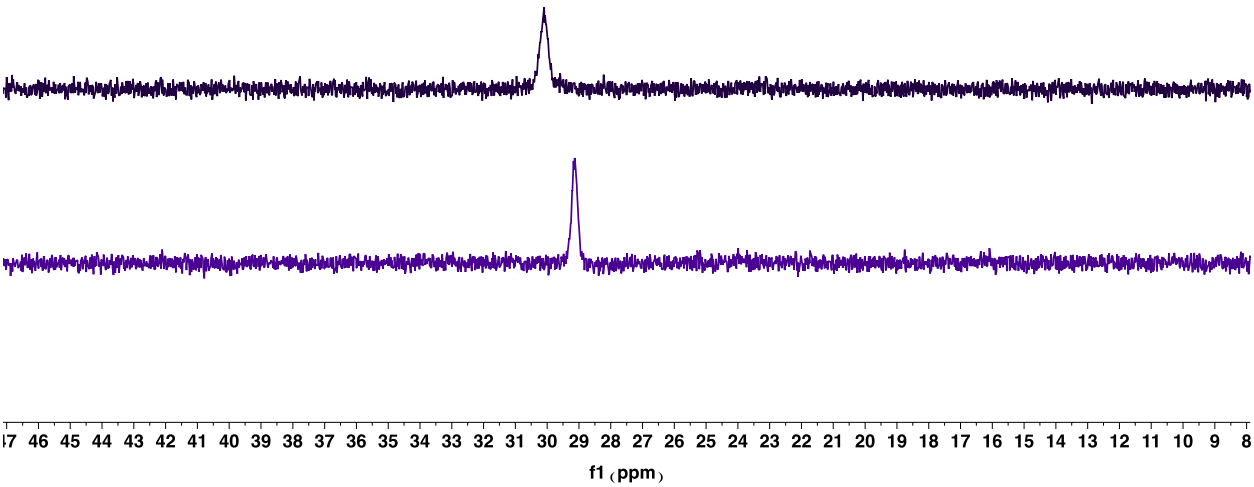

Figure S31. $^{31}P\{^{1}H\}$ NMR spectra of the following in CD_2Cl_2: Bottom spectrum is $[(PPh_3)Au][OTf]$ with 1 eq of pyridine. Top spectrum is $[(PPh_3)Au][OTf]$ in the absence of pyridine.

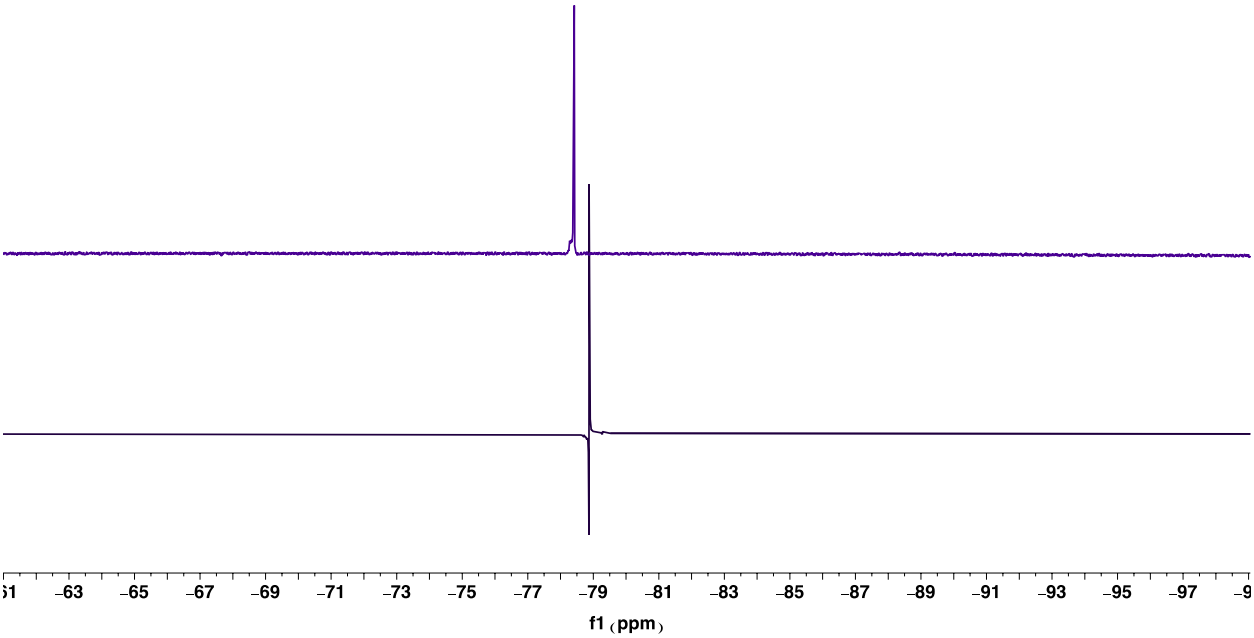

Figure S32. $^{19}F\{^{1}H\}$ NMR spectra of the following in CD_2Cl_2: Bottom spectrum is $[Au(PPh_3)][OTf]$ with pyridine. Top spectrum is $[Au(PPh_3)][OTf]$ in the absence of pyridine.

CV Chromatograms of 1 and 1-F

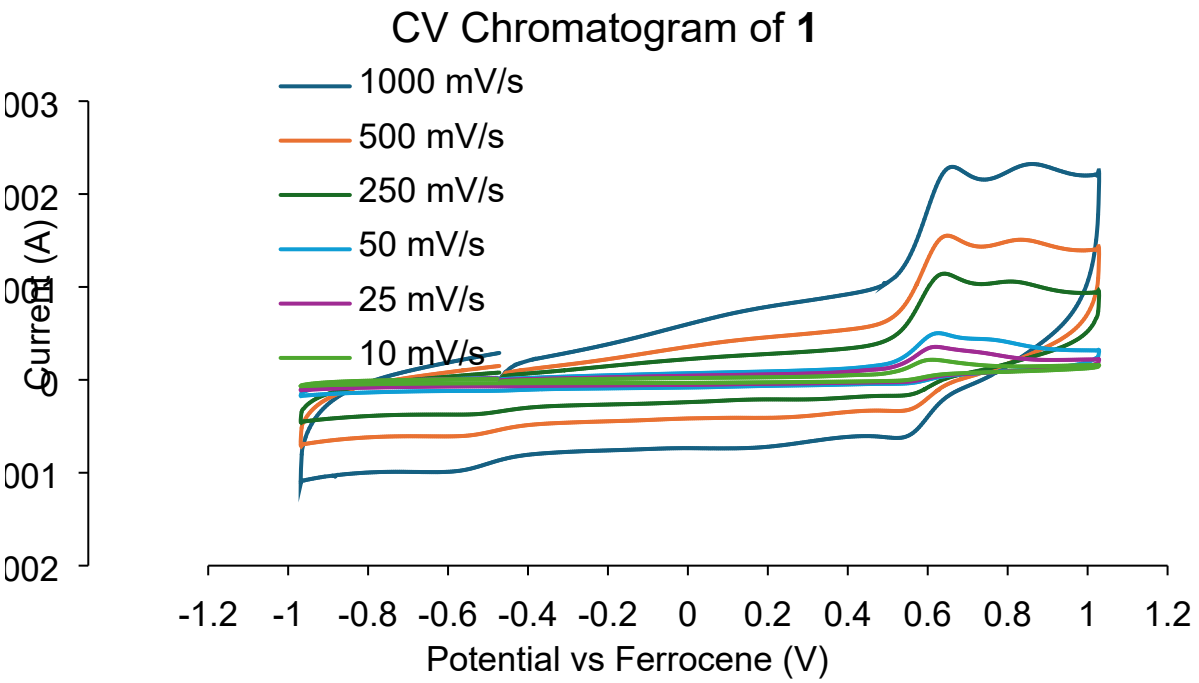

Figure S33. Cyclic voltammetry chromatogram of **1** in DCM with 100 mM tetrabutyl ammonium hexafluorophosphate used as electrolyte. CVs were performed by scanning in the oxidative direction first. Scan rates were varied from 10 mV/s to 1,000 mV/s.

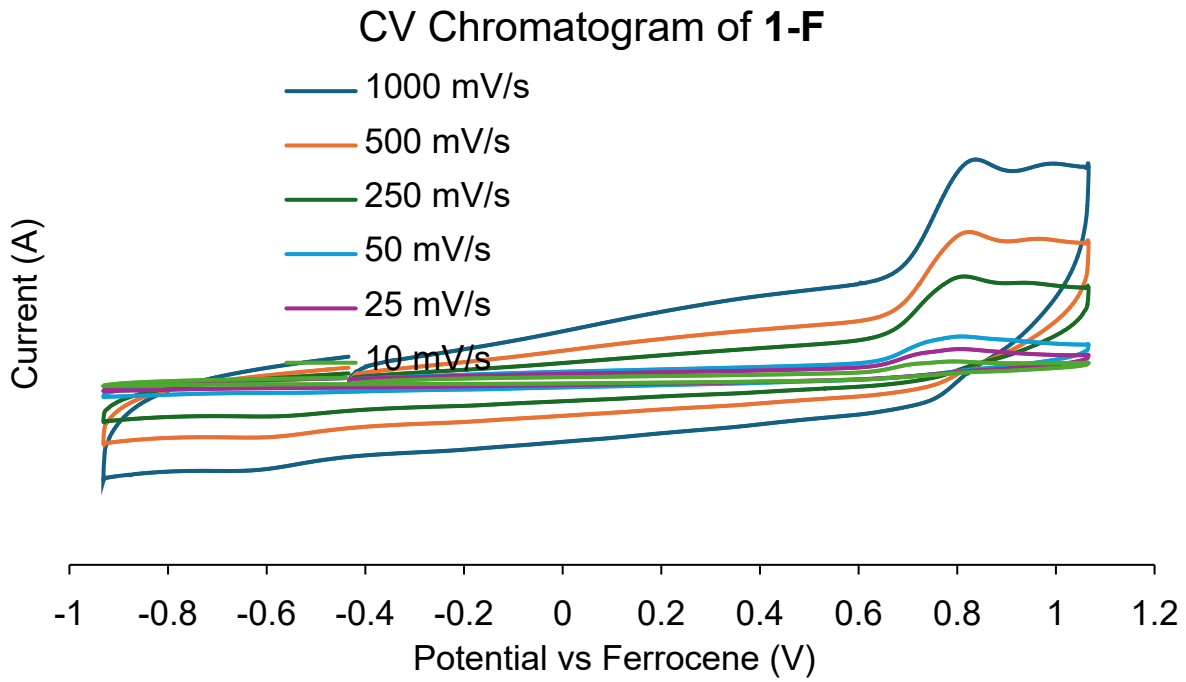

Figure S34. Cyclic voltammetry chromatogram of **1-F** in DCM with 100 mM tetrabutyl ammonium hexafluorophosphate used as electrolyte. CVs were performed by scanning in the oxidative direction first. Scan rates were varied from 10 mV/s to 1,000 mV/s.

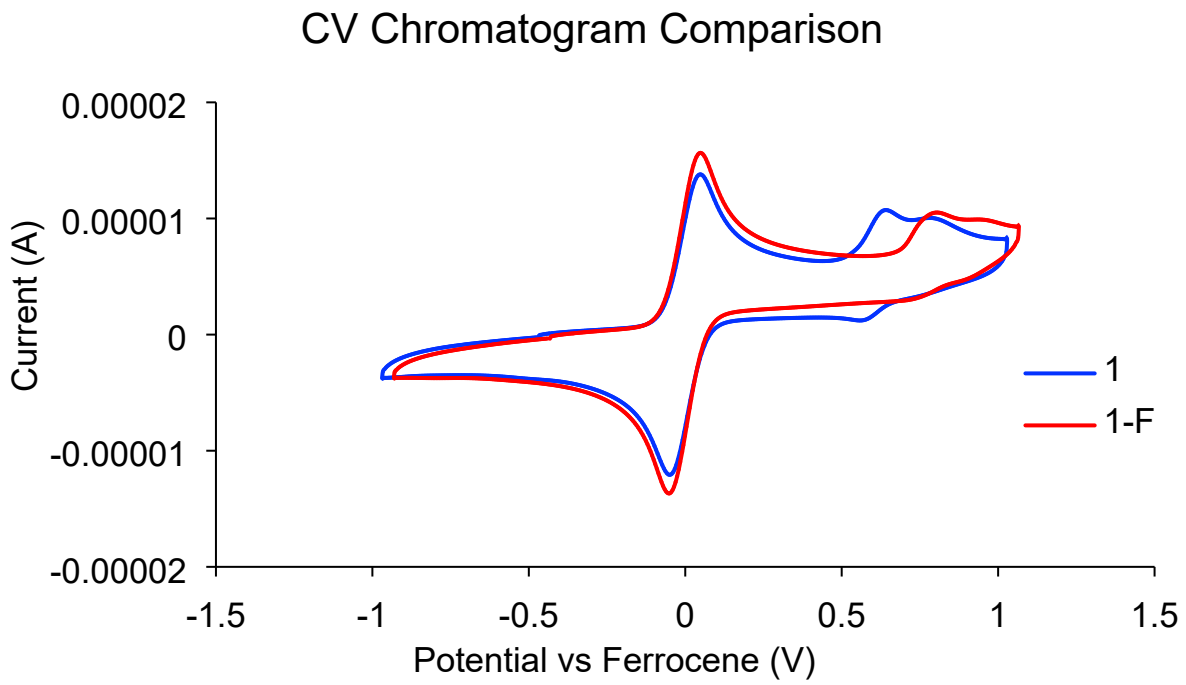

Figure S35. Cyclic voltammetry comparison of **1** and **1-F** in DCM with 100 mM tetrabutyl ammonium hexafluorophosphate used as electrolyte. Scan rate for this comparison was 100 mV/s. Ferrocene is also present in these chromatograms. CVs were performed by scanning in the oxidative direction first.

Plots of normalized ppm change of 2 and 2-F vs equivalents of titrant

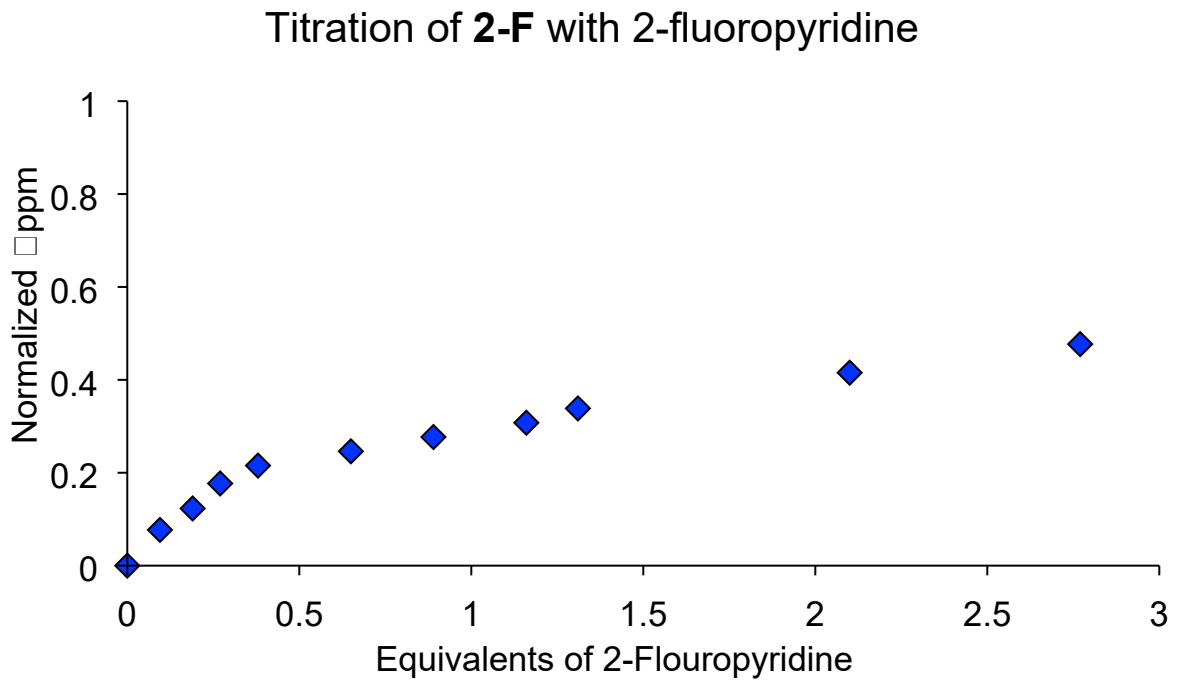

Figure S36. Plot of normalized ∆ppm vs equivalents of 2-fluoropyridine in the titration of **2-F** with 2-fluoropyridine. Herein, the value of 0 in "normalized ∆ppm" is the chemical shift of the proton alpha to Pt in **2-F**. The value of 1 in "normalized ∆ppm" is the chemical shift of the proton alpha to Pt in **1-F**.

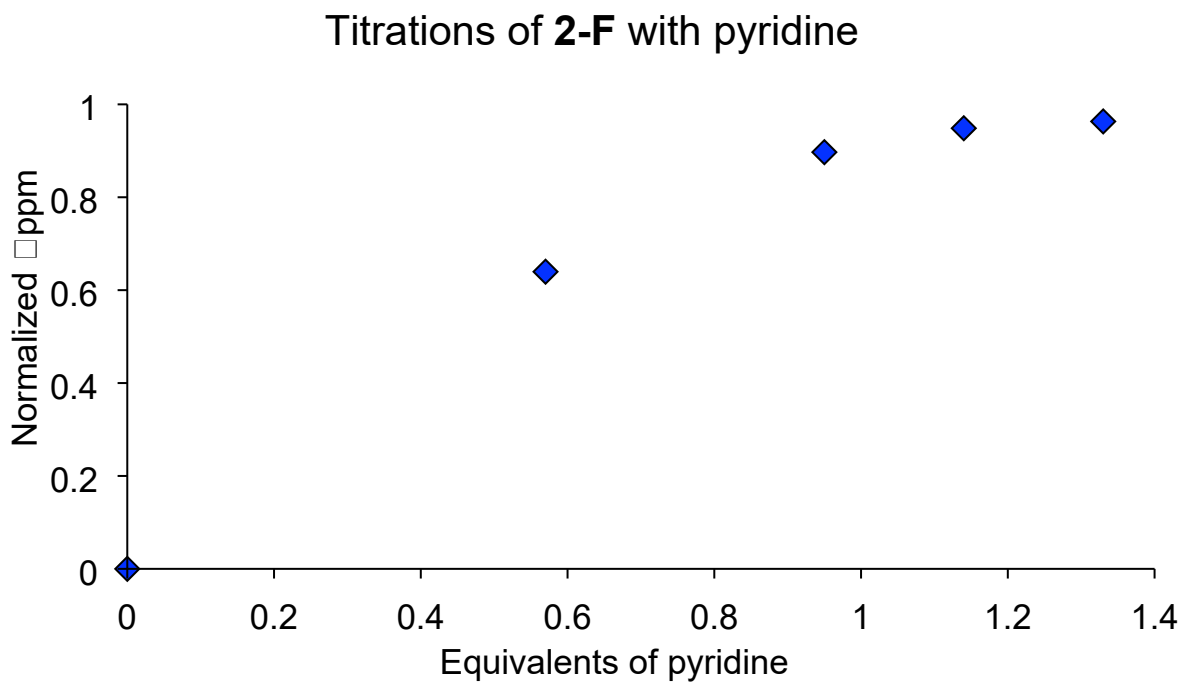

Figure S37. Plot of normalized ∆ppm vs equivalents of pyridine in the titration of **2-F** with pyridine. Herein, the value of 0 in "normalized ∆ppm" is the chemical shift of the proton alpha to Pt in **2-F**. The value of 1 in "normalized ∆ppm" is the chemical shift of the proton alpha to Pt in **1-F**.

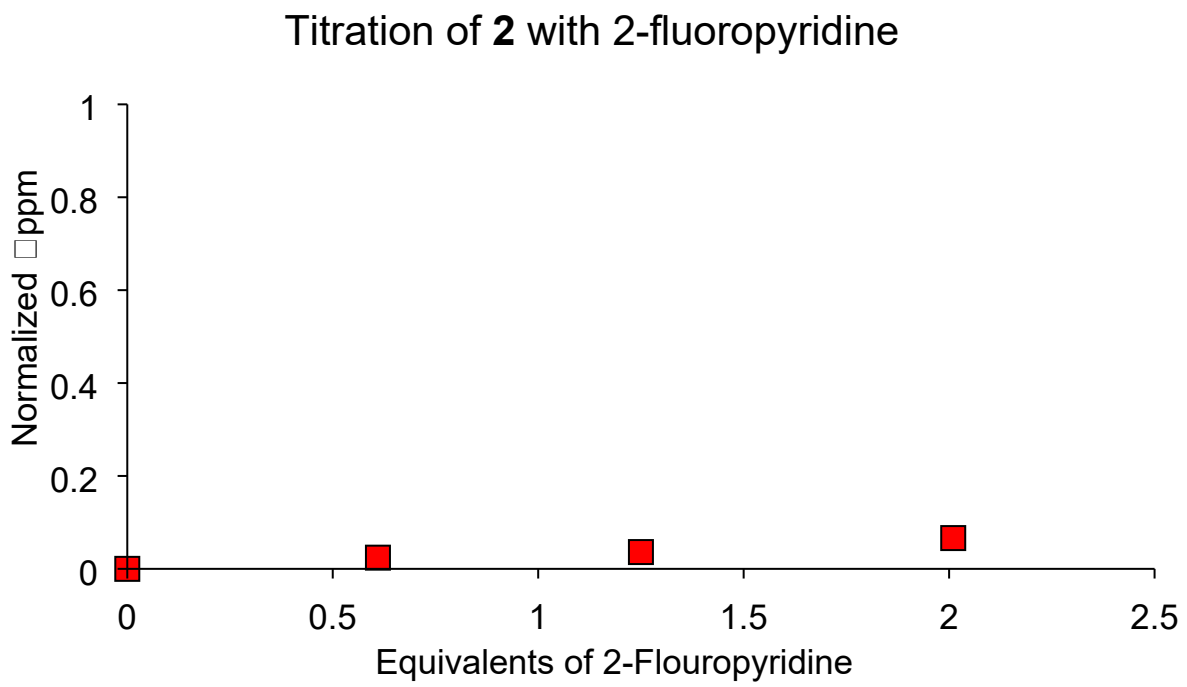

Figure S38. Plot of normalized ∆ppm vs equivalents of 2-fluoropyridine in the titration of **2** with 2-fluoropyridine. Herein, the value of 0 in "normalized ∆ppm" is the chemical shift of the proton alpha to Pt in **2**. The value of 1 in "normalized ∆ppm" is the chemical shift of the proton alpha to Pt in **1**.

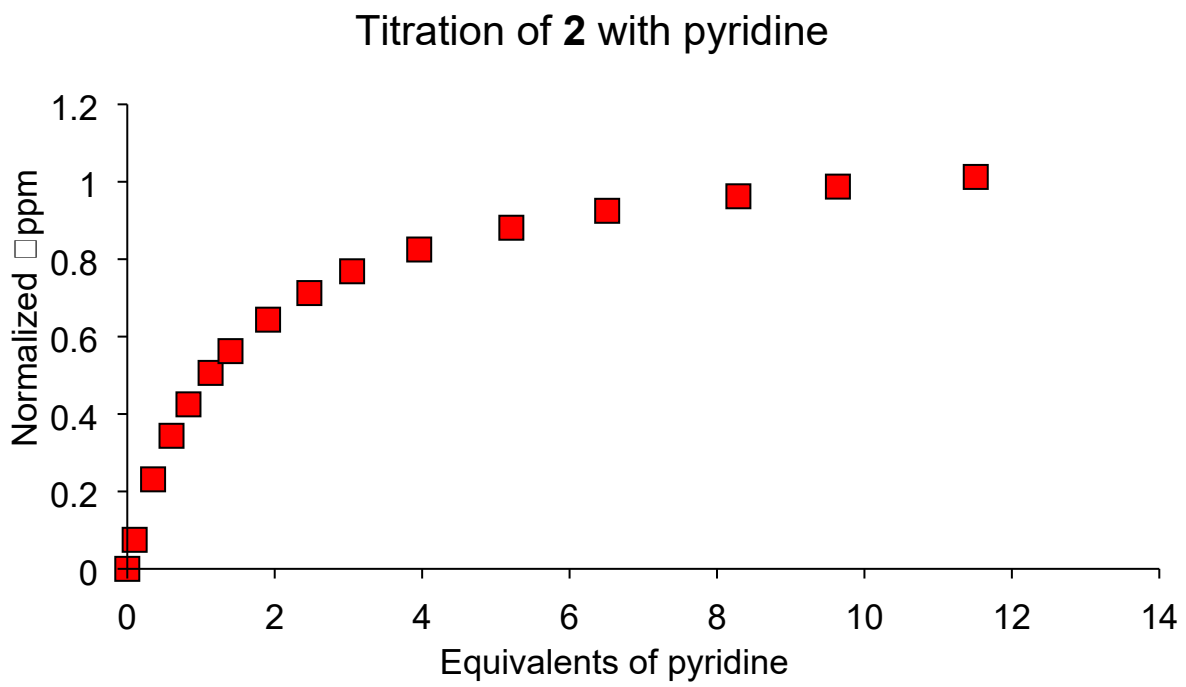

Figure S39. Plot of normalized Δppm vs equivalents of pyridine in the titration of **2** with pyridine. Herein, the value of 0 in "normalized Δppm" is the chemical shift of the proton alpha to Pt in **2**. The value of 1 in "normalized Δppm" is the chemical shift of the proton alpha to Pt in **1**.

Estimating K_{eq} using ^{1}H NMR data

Rapidly equilibrating species in solution, with respect to the NMR time scale, will have a chemical shift that is an average of the two separate species. For example, the chemical shift of species A changes as X is added and some amount of AX is generated in solution.

$$A + X \rightleftharpoons AX$$

Specifically, the chemical shift observed at equilibrium under conditions were AX and A undergo rapid, reversible exchange will be a mole-fraction weighted average of the separate chemical shifts according to the following equation.[8,9]

$$\partial_{obs} = N_A\partial_A + N_{AX}\partial_{AX}$$

Equation S1. The observed chemical shift at equilibrium based on the mole fraction of A and AX as well as the chemical shift of A and AX.

In this equation, ∂_{obs} is the observed chemical shift under equilibrating conditions, N_A is the mole fraction of A at equilibrium, N_{AX} is the mole fraction of AX at equilibrium, ∂_A is the chemical shift of A, and ∂_{AX} is the chemical shift of AX. When one considers that the concentration of A + AX is equal to the initial concentration of A added to the NMR solution, the ∂_{obs} can be used to calculate the concentration of A and AX. With those concentrations in hand, one can calculate the equilibrium constant (K_{eq}).

Specifically, the equilibrium being observed in this report is the reaction of pyridine (or 2-fluoropyridine) with the dinuclear complexes **2** and **2-F** (Scheme S1).

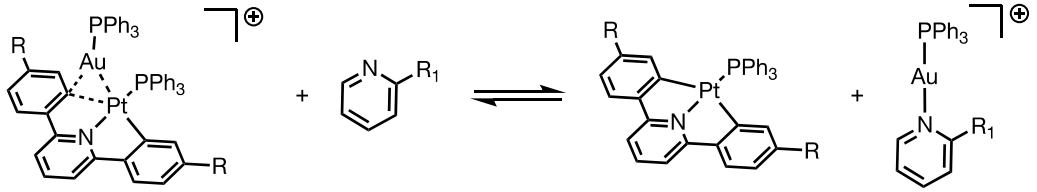

Scheme S1. Titrations of **2** (R = H) and **2-F** (R = F) with pyridine (R_1 = H) and 2-fluoropyridine (R_1 = F) to generate **1** (R = H) and **1-F** (R = F) and a pyridine ligated gold cationic species.

As a simplification, we treat this reaction as a pyridine binding event only (i.e. we treat this as A + X in equilibrium with AX). With this simplification, the dinuclear complex **2** or **2-F** is treated as A, pyridine is treated as X, and the monometallic Pt-species (**1** or **1-F**) is treated as AX. The values for ∂_A and ∂_{AX} are known as these are the chemical shift values for **2** or **2-F** and **1** or **1-F**. We then use the Solver add-in for Excel to determine the concentration of AX by minimizing the sum of square deviations between the ∂_{obs} and ∂_{calc} when using different equivalents of pyridine for titrations. The concentration of AX of each titration experiment was then used to calculate the K_{eq}. The K_{eq} calculated for each titration experiment was then averaged to give the final value (see Tables S1 – S4).

The accuracy of these equilibrium constants, as described by Drago,[9] requires that the chemical shift be "shifted considerably" upon binding of X. Here, the chemical shift change is ~ 0.2 ppm upon displacement of the $[(PPh_3)Au]^+$, which may contribute some error in the determination of K_{eq}. Also, broadening in the ^{1}H NMR spectrum, in particular with **2-F** titration experiments, leads

to small uncertainties in determining the chemical shift of the protons under consideration. While broadening alone would only partially contribute to error in determining K_{eq}, the combination of broadening and the small Δppm on displacement of $[(PPh_3)Au]^+$ may lead to a larger amount of error. However, while the absolute K_{eq} may be difficult to determine with high accuracy in these experiments, we believe the order of magnitude of the determined K_{eq} is accurate. Thus, we can conclude that the $[(PPh_3)Au]^+$ of **2-F** is more readily displaced by pyridine and 2-fluoropyridine than the $[(PPh_3)Au]^+$ of **2** by 2 orders of magnitude.

Table S1. Data and calculation for the titration of **2-F** with 2-fluoropyridine. Here, the initial concentrations of X (2-fluoropyridine) and A (**2-F**) are known. The ∂A is the chemical shift of **2-F**, and ∂AX is the chemical shift of **1-F**. The $[AX]_f$, the concentration of **1-F** at equilibrium, is determined using Excel's Solver by minimizing the sum of square deviation between the ∂_{obs} and the calculated ∂_{obs}. The $[AX]_f$ can then be used to calculate the K_{eq}; the K_{eq} for each addition of 2-fluoropyridine is averaged to give K_{eq} used in the manuscript.

	∂A	**5.69**	**∂AX**	**5.82**			**Average K_{eq}**
$[X]_0$	**∂_{obs}**	**$[A]_0$**	**$[AX]_f$**	**∂_{obs}(calc)**	**$(\Delta(\partial_{obs} - \partial_{obs}(calc)))^2$**	**K_{eq}**	**1.29**
0.00	5.69	1.00	0.00	5.69	0.00E+00		
0.19	5.71	1.00	0.14	5.71	1.28E-16	3.23	
0.27	5.71	1.00	0.19	5.71	2.67E-16	3.00	
0.38	5.72	1.00	0.23	5.72	2.37E-16	1.94	
0.65	5.72	1.00	0.26	5.72	9.11E-17	0.88	
0.89	5.73	1.00	0.29	5.73	1.36E-17	0.67	
1.16	5.73	1.00	0.32	5.73	4.82E-18	0.55	
1.31	5.73	1.00	0.35	5.73	6.48E-17	0.55	
2.10	5.74	1.00	0.42	5.74	5.14E-16	0.43	
2.77	5.75	1.00	0.48	5.75	1.18E-15	0.40	
				SSD =	2.50E-15		

Table S2. Data and calculation for the titration of **2** with 2-fluoropyridine. Here, the initial concentrations of X (2-fluoropyridine) and A (**2**) are known. The ∂A is the chemical shift of **2**, and ∂AX is the chemical shift of **1**. The $[AX]_f$, the concentration of **1** at equilibrium, is determined using Excel's Solver by minimizing the sum of square deviation between the ∂_{obs} and the calculated ∂_{obs}. The $[AX]_f$ can then be used to calculate the K_{eq}; the K_{eq} for each addition of 2-fluoropyridine is averaged to give K_{eq} used in the manuscript.

	∂A	**6.07**	**∂AX**	**6.23**			**Average K_{eq}**
$[X]_0$	**∂_{obs}**	**$[A]_0$**	**$[AX]_f$**	**∂_{obs}(calc)**	**$(\Delta(\partial_{obs} - \partial_{obs}(calc)))^2$**	**K_{eq}**	**0.04**
0.00	6.23	1.00	1.00	6.23	2.12E-17		
0.61	6.07	1.00	0.02	6.07	6.05E-15	0.04	
1.25	6.08	1.00	0.04	6.08	5.86E-15	0.03	
2.01	6.08	1.00	0.07	6.08	5.48E-15	0.04	
				SSD =	1.74E-14		

Table S3. Data and calculation for the titration of **2-F** with pyridine. Here, the initial concentrations of X (pyridine) and A (**2-F**) are known. The ∂A is the chemical shift of **2-F**, and ∂AX is the chemical shift of **1-F**. The $[AX]_f$, the concentration of **1-F** at equilibrium, is determined using Excel's Solver by minimizing the sum of square deviation between the ∂_{obs} and the calculated ∂_{obs}. The $[AX]_f$ can then be used to calculate the K_{eq}; the K_{eq} for each addition of pyridine is averaged to give K_{eq} used in the manuscript.

	∂A	**5.69**	**∂AX**	**5.82**			**Average K_{eq}**
$[X]_0$	**∂_{obs}**	**$[A]_0$**	**$[AX]_f$**	**∂_{obs}(calc)**	**$(\Delta(\partial_{obs} - \partial_{obs}(calc)))^2$**	**K_{eq}**	**110**
0.00	5.69	1.00	0.00	5.69	0.00E+00		
0.95	5.81	1.00	0.90	5.81	1.18E-14	164.60	
1.14	5.82	1.00	0.95	5.82	5.25E-15	96.25	
1.33	5.82	1.00	0.96	5.82	1.72E-14	71.43	
				SSD =	3.42E-14		

Table S4. Data and calculation for the titration of **2** with pyridine. Here, the initial concentrations of X (pyridine) and A (**2**) are known. The ∂A is the chemical shift of **2**, and ∂AX is the chemical shift of **1**. The $[AX]_f$, the concentration of **1** at equilibrium, is determined using Excel's Solver by minimizing the sum of square deviation between the ∂_{obs} and the calculated ∂_{obs}. The $[AX]_f$ can then be used to calculate the K_{eq}; the K_{eq} for each addition of pyridine is averaged to give K_{eq} used in the manuscript.

	∂A	**6.07**	**∂AX**	**6.23**			**Average K_{eq}**
$[X]_0$	**∂obs**	**$[A]_0$**	**$[AX]_f$**	**∂obs(calc)**	**$(\Delta(\partial_{obs} - \partial_{obs}(calc)))^2$**	**K_{eq}**	2.00
0.00	6.07	1.00	0.00	6.07	0.00E+00		
0.10	6.08	1.00	0.07	6.08	3.06E-16	3.24	
0.35	6.11	1.00	0.23	6.11	1.59E-14	2.53	
0.60	6.13	1.00	0.34	6.12	2.66E-14	2.04	
0.83	6.14	1.00	0.42	6.14	8.75E-14	1.82	
1.13	6.15	1.00	0.51	6.15	4.24E-15	1.64	
1.40	6.16	1.00	0.56	6.16	5.26E-14	1.54	
1.91	6.17	1.00	0.64	6.17	6.27E-15	1.43	
2.47	6.18	1.00	0.71	6.18	9.50E-14	1.41	
3.05	6.19	1.00	0.77	6.19	1.08E-13	1.46	
3.96	6.20	1.00	0.82	6.20	1.45E-13	1.50	
5.21	6.21	1.00	0.88	6.21	2.20E-13	1.71	
6.51	6.22	1.00	0.92	6.22	2.88E-13	2.21	
8.29	6.22	1.00	0.96	6.22	6.05E-13	3.50	
				SSD =	1.65E-12		

X-ray crystal structure of 2-F

Crystals suitable for single crystal X-ray diffraction were obtained by slow diffusion of pentane into a DCM solution of **2-F**.

Data collection: APEX5 (Bruker, 2016); cell refinement: SAINT V8.40A (Bruker, 2019); data reduction: SAINT V8.40A (Bruker, 2019); program used to solve structure: SHELXT;[10] program used to refine structure: SHELXL 2018/3;[10] molecular graphics: Olex2 1.5 (Dolomanov et al., 2009);[11] software used to prepare material for publication: Olex2 1.5 (Dolomanov et al., 2009).[11]

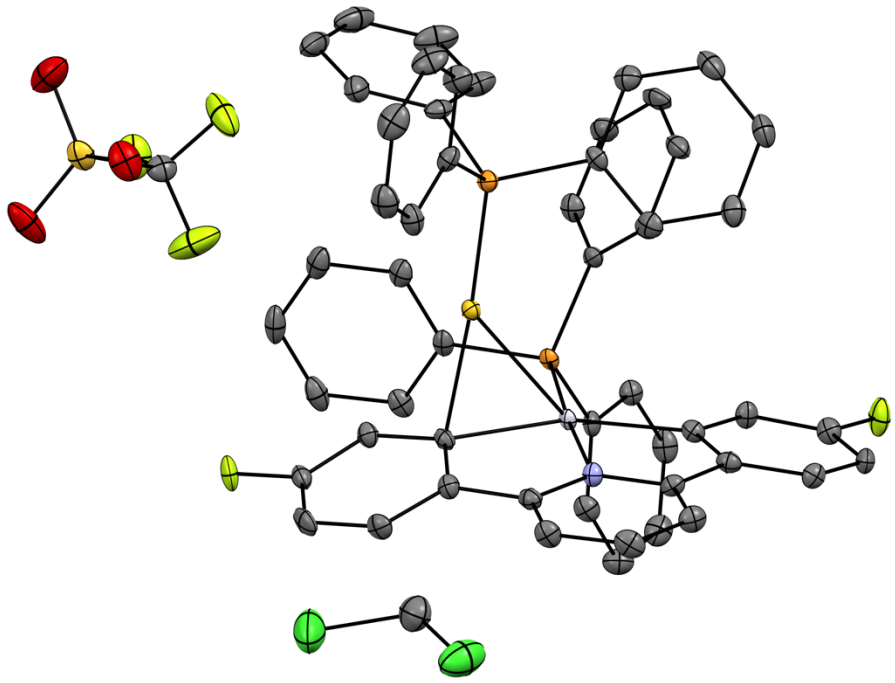

Figure S40. Molecular structure of **2-F** with a molecule of DCM. Hydrogens are omitted for clarity. Thermal ellipsoids are shown at the 50% probability level

Crystal data

$C_{53}H_{39}AuF_2NP_2Pt \cdot CF_3O_3S \cdot CH_2Cl_2$	Z = 2
M_r = 1415.84	F(000) = 1368
Triclinic, $P\bar{1}$	D_x = 1.884 Mg m^{-3}
a = 11.8472 (11) Å	Cu Ka radiation, l = 1.54178 Å
b = 13.4093 (12) Å	Cell parameters from 9181 reflections
c = 16.6730 (15) Å	q = 3.4–66.6°
a = 76.964 (2)°	m = 13.14 mm^{-1}
b = 75.349 (2)°	T = 100 K
g = 86.149 (2)°	Irregular, clear orange
V = 2496.4 (4) Å^3	0.20 × 0.18 × 0.13 mm

Data collection

Bruker D8 Venture diffractometer	8723 independent reflections
Radiation source: Microfocus Sealed Tube	8706 reflections with $I > 2s(I)$
Helios Cu monochromator	R_{int} = 0.044
f and w scans	q_{max} = 66.6°, q_{min} = 2.8°
Absorption correction: numerical *SADABS2016*/2 (Bruker,2016/2) was used for absorption correction. wR2(int) was 0.1333 before and 0.0769 after correction. The Ratio of minimum to maximum transmission is 0.4290. The l/2 correction factor is Not present.	*h* = -14Æ14
T_{min} = 0.182, T_{max} = 0.425	*k* = -15Æ15
69643 measured reflections	*l* = -19Æ19

Refinement

Refinement on F^2	0 restraints
Least-squares matrix: full	Hydrogen site location: inferred from neighbouring sites
$R[F^2 > 2\sigma(F^2)]$ = 0.028	H-atom parameters constrained
$wR(F^2)$ = 0.073	$w = 1/[\sigma^2(F_o^2) + (0.0334P)^2 + 10.3056P]$ where $P = (F_o^2 + 2F_c^2)/3$
S = 1.13	$(\Delta/\sigma)_{max}$ = 0.003
8723 reflections	$\Delta\rho_{max}$ = 0.96 e Å^{-3}
640 parameters	$\Delta\rho_{min}$ = -1.70 e Å^{-3}

Other details

Geometry. All esds (except the esd in the dihedral angle between two l.s. planes) are estimated using the full covariance matrix. The cell esds are taken into account individually in the estimation of esds in distances, angles and torsion angles; correlations between esds in cell parameters are only used when they are defined by crystal symmetry. An approximate (isotropic) treatment of cell esds is used for estimating esds involving l.s. planes.

Computational details

The Density Functional Theory (DFT) studies carried out in this manuscript were performed using the Gaussian 16 program.[12] For geometry optimizations, calculations were performed in the gas phase with the B3LYP functional and a split basis set, LANL2DZ for Pt atoms and 6-31G(d) for all other atoms. The crystal structures for **1**[1] and **1-F**[2] were used as starting points for these geometry optimizations. The coordinates for the optimized structures of **1** and **1-F** are included with this submission as .xyz files. The optimized geometries for **1** and **1-F** were used for molecular orbital calculations also using the Gaussian 16 program. For these molecular orbital calculations, multiple functionals were tested (B3LYP, PBE, PBE0, and M06). The same split basis sets were used for each functional; LANL2DZ for Pt atoms and 6-311+G(2d,p) for all other atoms. The molecular orbitals were visualized using the Gaussian 16 program and the HOMOs for **1** and **1-F** using each functional are shown below.

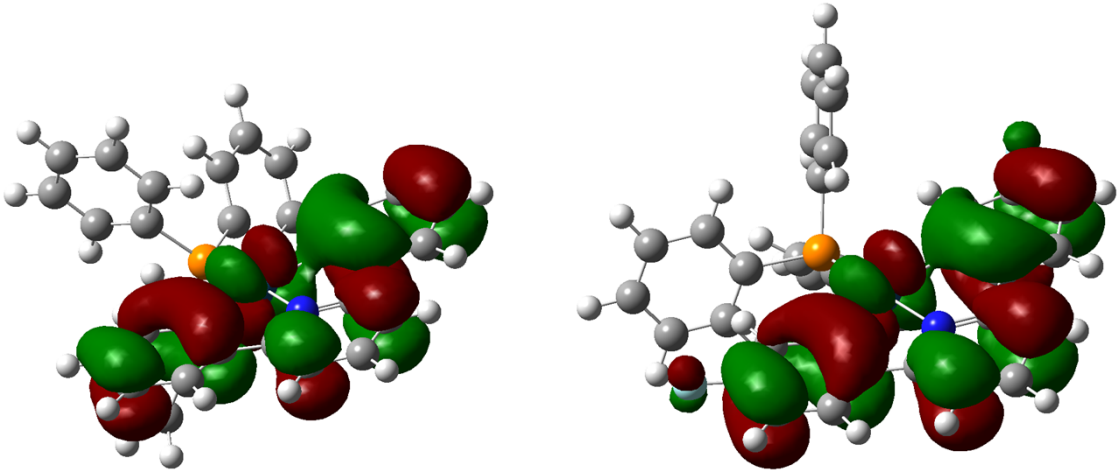

Figure S41. The HOMO for **1** (left) and **1-F** (right) using the B3LYP functional.

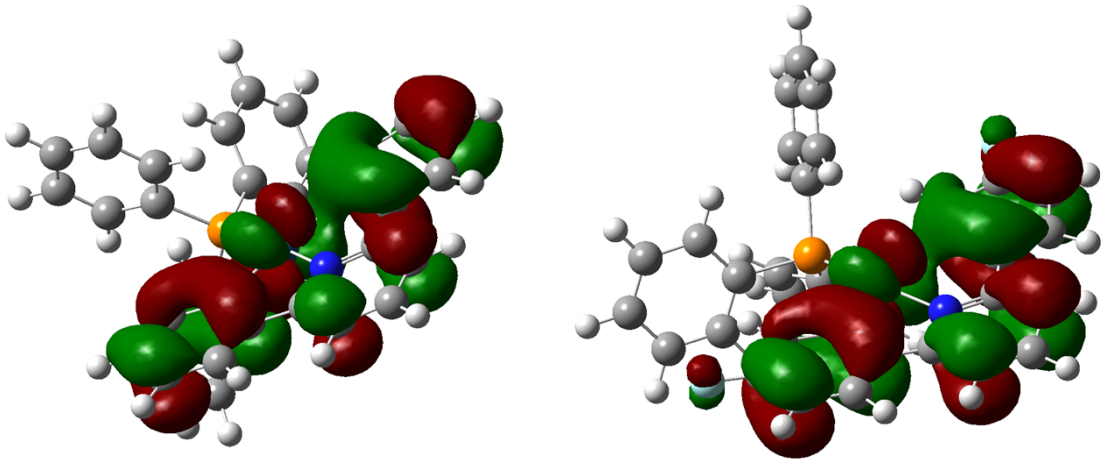

Figure S42. The HOMO for **1** (left) and **1-F** (right) using the PBE functional.

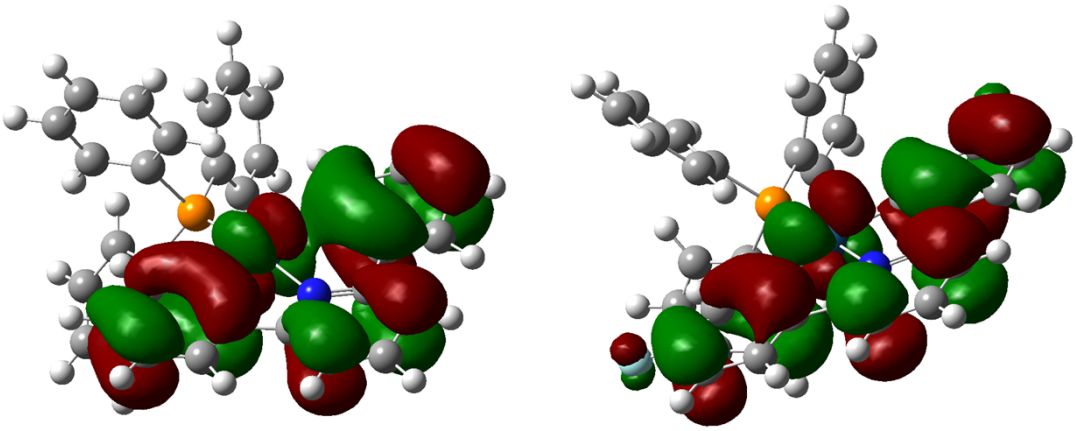

Figure S43. The HOMO for **1** (left) and **1-F** (right) using the PBE0 functional.

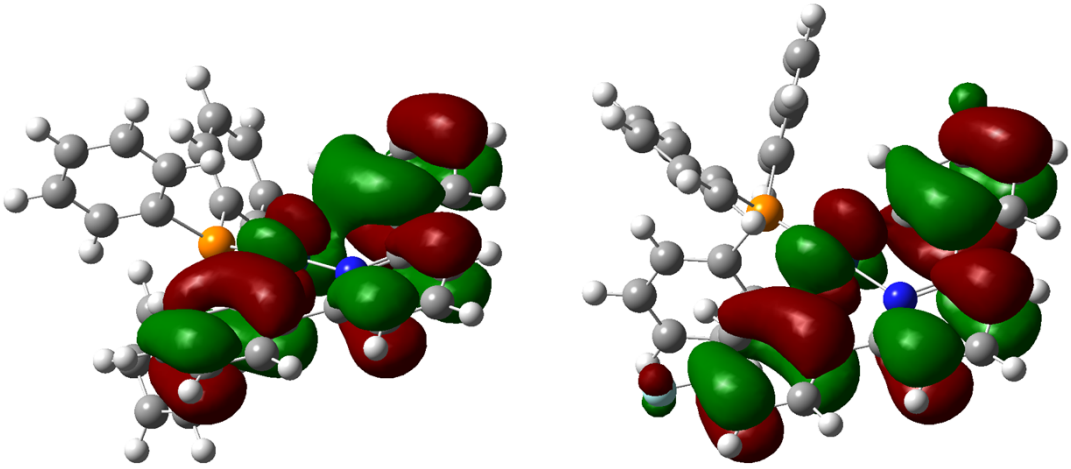

Figure S44. The HOMO for **1** (left) and **1-F** (right) using the M06 functional.

References

1. Baya, M.; Belio, U.; Fernandez, I.; Fuertes, S.; Martin, A. Unusual Metal-Metal Bonding in a Dinuclear Pt-Au Complex: Snapshot of a Transmetalation Process. *Angew. Chem. Int. Ed. Engl.* **2016**, *55*, 6978-6982
2. Shaw, P. A.; Phillips, J. M.; Clarkson, G. J.; Rourke, J. P. Trapping five-coordinate platinum(iv) intermediates. *Dalton Trans.* **2016**, *45*, 11397-11406
3. Pauli, G. F.; Chen, S.-N.; Simmler, C.; Lankin, D. C.; Gödecke, T.; Jaki, B. U.; Friesen, J. B.; McAlpine, J. B.; Napolitano, J. G., Importance of Purity Evaluation and the Potential of Quantitative ^{1}H NMR as a Purity Assay. *J. Med. Chem.* **2014**, *57*, 9220-9231
4. Pauli, G. F.; Gödecke, T.; Jaki, B. U.; Lankin, D. C., Quantitative ^{1}H NMR. Development and Potential of an Analytical Method: An Update. *J. Nat. Prod.* **2012**, *75*, 834-851
5. Mahajan, S.; Singh, I. P., Determining and reporting purity of organic molecules: why qNMR. *Magn. Reson. Chem*. **2013**, *51*, 76-81
6. Webster, G. K., Expanding the Analytical Toolbox: Pharmaceutical Application of Quantitative NMR. *Anal. Chem.* **2014**, *86*, 11474-11480
7. Beamer, A. W.; Buss, J. A. Synthesis, Structural Characterization, and CO2 Reactivity of a Constitutionally Analogous Series of Tricopper Mono-, Di-, and Trihydrides *J. Am. Chem. Soc.*, **2023**, *145*, 12911-12919
8. Drago, R. S., Physical Methods for Chemists. 2nd ed.; Surfside Scientific Publishers: Gainesville, FL, pp 290-291
9. Parks, D. J.; Piers, W. E., Tris(pentafluorophenyl)boron-Catalyzed Hydrosilation of Aromatic Aldehydes, Ketones, and Esters. *J. Am. Chem. Soc.*, **1996**, *118*, 9440-9441
10. Sheldrick, G. M. Crystal Structure Refinement with SHELXL *Acta Cryst.* **2015**, *71*, 3-8
11. Dolomanov, O. V.; Bourhis, L. J.; Gildea, R. J.; Howard, J. A. K.; Puschmann, H. OLEX2: A complete structure solution, refinement and analysis program. *J. Appl. Cryst.* **2009**, *42*, 339-341
12. Gaussian 16 M. J. Frisch, G. W. Trucks, H. B. Schlegel, G. E. Scuseria, M. A. Robb, J. R. Cheeseman, G. Scalmani, V. Barone, G. A. Petersson, H. Nakatsuji, X. Li, M. Caricato, A. V. Marenich, J. Bloino, B. G. Janesko, R. Gomperts, B. Mennucci, H. P. Hratchian, J. V. Ortiz, A. F. Izmaylov, J. L. Sonnenberg, Williams, F. Ding, F. Lipparini, F. Egidi, J. Goings, B. Peng, A. Petrone, T. Henderson, D. Ranasinghe, V. G. Zakrzewski, J. Gao, N. Rega, G. Zheng, W. Liang, M. Hada, M. Ehara, K. Toyota, R. Fukuda, J. Hasegawa, M. Ishida, T. Nakajima, Y. Honda, O. Kitao, H. Nakai, T. Vreven, K. Throssell, J. A. Montgomery Jr., J. E. Peralta, F. Ogliaro, M. J. Bearpark, J. J. Heyd, E. N. Brothers, K. N. Kudin, V. N. Staroverov, T. A. Keith, R. Kobayashi, J. Normand, K. Raghavachari, A. P. Rendell, J. C. Burant, S. S. Iyengar, J. Tomasi, M. Cossi, J. M. Millam, M. Klene, C. Adamo, R. Cammi, J. W. Ochterski, R. L. Martin, K. Morokuma, O. Farkas, J. B. Foresman, D. J. Fox, Gaussian, Inc., Wallingford CT, **2016**.